ISSN 0972-0480 • Vol. 26 No. 6 • June 2023

IIM METAL NEWS

A monthly publication of The Indian Institute of Metals

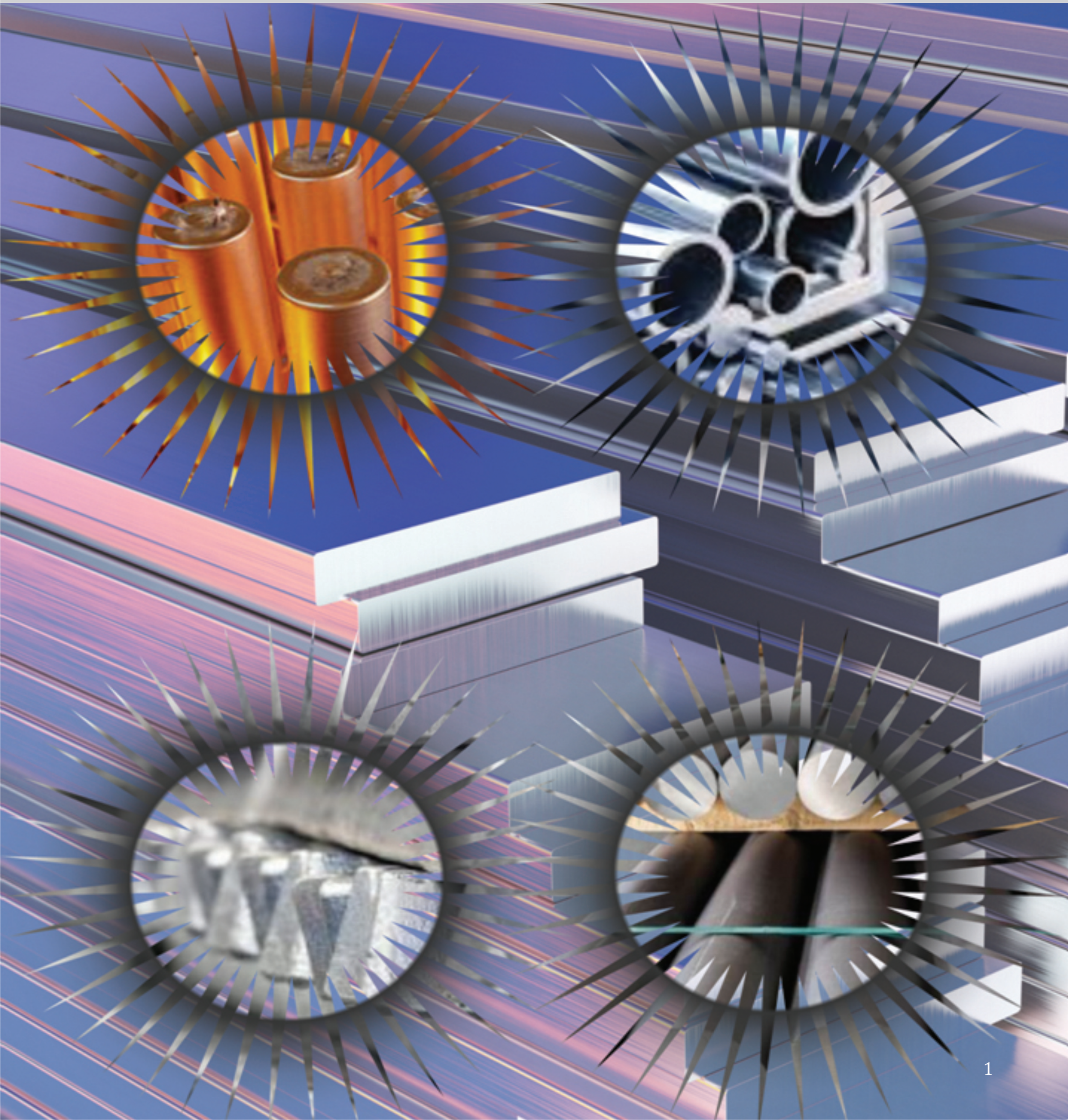

IIM METAL NEWS

Vol. 26 No. 6 June 2023

Chief Editor
Dr K Bhanu Sankara Rao

Printed and Published by
Shri Bhaskar Roy, Acting Secretary General, on behalf of "The Indian Institute of Metals", and
printed at Print Max, 44, Biplabi Pulindas Street, Kolkata-700009 and
published at 'Metal House', Plot 13/4, Block AQ, Sector V, Salt Lake, Kolkata-700091, West Bengal, India

E-mail: thesecretarygeneral.iim@gmail.com, iimmetalnews@yahoo.com
Phone: 033-2367 9768 / 2367 5004
Website: www.iim-india.net
Fax: (033) 2367 5335
Facebook - https://www.facebook.com TheIndianInstituteofMetals/
Instagram - https://www.instagram.com/indianinstituteofmetals/
LinkedIn - https://www.linkedin.com/company/the-indian-institute-of-metals/
Twitter - https://twitter.com/iimetals_india

First row right side onward, Prof. B S Murty, Mr. Satish Pai, Dr. Samir V Kamat, Dr. U Kamachi Mudali;
Second row right side onward, Mr. Bhaskar Roy, Ms. Atashi Saha, Dr. D De Sarkar, Mr. Somnath Guha
@ Metal House, IIM-HO on 19.6.23

THE INDIAN INSTITUTE OF METALS

Technical Article

State-of-the-art in Laser Powder Bed Fusion of Aluminium Alloys

K S N Satish Idury[a], R L Narayan[b]

Abstract

The fabrication of Aluminium (Al) alloys through laser powder bed fusion (LPBF) offers immense promise in terms of near net shaped manufacturing and remarkable control over process parameters that can be tuned to obtain a desired mechanical performance. While cast Al alloys are easily printable, wrought Al alloys pose serious challenges during LPBF and are susceptible to cracking and profuse defect formation. Here, a detailed review of contemporary strategies to enhance printability and mitigation of defects in LPBF processed Al alloys is provided. First the role of grain refinements and computational alloy design approaches in enhancing the printability of Al alloys is critically discussed. Thereafter, the physical mechanisms of defect formation in Al alloys are reviewed and the key strategies in obviating defects are highlighted. We then summarize the role of various post process heat treatments and outline the peculiarities and remarkable opportunities provided by LPBF processed Al alloys for attaining unique microstructural attributes including enhancing their fatigue strength. Finally, we outline the generic strategies aimed at enhancing the fatigue life of LPBF processed Al alloys.

Key words: Aluminum alloys, laser powder bed fusion, printability, defects, fatigue.

1. Introduction

Aluminium alloys are widely used in several structural applications due to their high strength-to-weight ratio, good shape forming ability/machinability and excellent corrosion resistance [1]. Moreover, they are not only 100% recyclable, but their production has become 75% more energy efficient over time, which has earned them the reputation of being eco-friendly alloys [1, 2]. Al alloys are broadly categorized as wrought and cast varieties, on the basis of how they are processed. Cast Al alloys, as their name suggests, are produced by casting and are often used for non-critical applications, owing to presence of casting defects in them and their relatively lower strength [3]. Most cast Al alloys contain significant amounts of (>11 wt.%) Si, which enhances the fluidity and castability of the alloy remarkably. Alternately, wrought alloys, which represent ~80-85 % of all Al alloys produced, are processed via conventional manufacturing routes such as forging, rolling, extrusion and are used for high-end aerospace and automotive applications [3,4]. Wrought Al alloys are further grouped into 8 series, referred to as 1xxx-8xxx, based on the primary element present in the alloy besides Al. Amongst these, the 2xxx, 6xxx and 7xxx series alloys are recognized as heat-treatable alloys, as precipitate strengthening in them can be achieved by performing appropriate age hardening. The other grades, namely the 1xxx, 3xxx and 5xxx series alloys, are not heat-treatable and can therefore only attain moderate strength, compared to the heat-treatable alloy grades, via cold working. 8000 series aluminium alloys are alloyed with other elements which are not covered by other series from 1xxx to 7xxx and an example is Aluminium–lithium alloys. Since the microstructure and mechanical behaviour of conventionally manufactured Al alloys are relatively well established, current studies on them focus on microalloying additions to incrementally fine tune their properties for specific applications. Besides these studies, there is profound interest in

[a] Department of Automation and Robotics
Sharad Institute of Technology College of Engineering Yadrav, Ichalkaranji – 416 115
[b] Department of Material Science and Engineering
Indian Institute of Technology Delhi, New Delhi – 110 016
E-mail : *rlnarayan@mse.iitd.ac.in*

developing and characterizing Al alloys using metal additive manufacturing (AM) methods.

AM methods are capable of fabricating near net shapes components using metal powders or wires as feedstock. These methods build virtually conceptualized structures iteratively with the help of a power source, such as laser or electron beam, that melts the feedstock material. The most popular of these methods, laser powder bed fusion (LPBF), has been customized to build different components using alloy powders [5, 6]. In LPBF, pockets of metal powder placed over a bed are selectively melted by a laser source, which results in the formation of millimetre sized melt-pools. Adjoining melt-pools on the same plane solidify and fuse together to form a 2D layer of the desired build. The vertical stacking and fusing of all such 2D layers results in the final component. Owing to the non-equilibrium nature of solidification in the melt-pool, sub-grains are formed within grains during solidification and some constituents segregate to the melt-pool boundaries. As a result, alloys manufactured with LPBF often have unique multi-scale hierarchical microstructures. From the preceding discussions, it is evident that fabricating different Al alloys via LPBF offers great opportunities not only in terms of near net shape manufacturing but also in tailoring the process parameters to develop unique microstructural attributes that can enhance their mechanical properties. While builds of some cast alloys like AlMgSi have been developed successfully with LPBF, fabricating most wrought alloy grades, barring the 4xxx series, has been challenging. Builds of these alloy grades contain cracks and/or contain large pores and defects. Some studies have identified the following three primary reasons for the poor processability of Al alloys via LPBF. First, most wrought alloys have a large freezing range which leads to liquid entrapment in the mushy zone followed by shrinkage. This leads to hot cracking of the builds. Second, there is only a tiny volume fraction of liquid available during the final stages of solidification that can fill the pores and cracks generated during LPBF [7-11]. Finally, builds are subjected to alternating heating and cooling cycles, which result in the development of tensile residual stresses in the build. These tensile residual stresses also cause the opening up of cracks during the final stage of solidification. The presence of such pores and cracks significantly deteriorates the fracture and fatigue strength of these builds. Therefore, in the context of developing Al alloys that can be fabricated with LPBF, the scientific community is confronted with the following questions. First, what process or material modifications can be implemented to enhance the printability of Al alloys? Second, can defects like pores, spatter and other anomalies be consistently eliminated in printed components? Third, what kind of post-build heat treatments can be implemented for tuning the microstructure of Al alloys? Finally, how can the fatigue life of components be enhanced in the presence of defects and pores. With specific emphasis on addressing the above-mentioned questions, this brief overview presents the state-of-the-art in LPBF fabrication of Al alloys.

2. Strategies to enhance LPBF processability of Al alloys

In LPBF, the thermal gradient (G) in the melt-pools promotes directional solidification, which initiates at the melt-pool boundaries and ends at the centre of the melt-pool. This leads to the formation of columnar grains whose axis is aligned with the build direction (vertical). The growth of columnar grains minimizes the ability of the melt to fill the pores and voids in the final stages of solidification, which induces hot cracking. To address this issue, conventional metallurgical approaches of adding grain refiners to the Al alloy or facilitating eutectic solidification of the alloy has been proposed. In the grain refinement strategy, the addition of Sc, Zr, Hf, Ti, and V elements facilitates the formation of $L1_2$ precipitates, such as Al_3Sc and Al_3Zr, that are coherent with the Al matrix [12-14]. Since these precipitates form during the early stages of solidification, they trigger heterogeneous nucleation of Al grains around them [15,16]. Heterogeneous nucleation promotes the growth of several grains at a much smaller degree of undercooling than that required in the absence of grain refiners. This strategy also facilitates columnar-to-equiaxed transition (CET), which has an added benefit of minimizing mechanical anisotropy in the build. In the eutectic solidification strategy, where eutectic forming Al-Si and Al-Ce systems are considered, the emphasis is on the formation of a low melting eutectic liquid during the final stage of solidification, which fills the pores and voids generated due to solidification shrinkage [7, 17-19].

Although both strategies have been reasonably successful in producing crack free builds of several Al alloy grades, they are fraught with some drawbacks, if pursued in isolation. First, grain refinement through addition of expensive elements like Sc and Zr is not preferred in industries that target large volume manufacturing. Second, the volume fraction of heterogeneous nucleation sites may not necessarily mitigate the formation of columnar grains in LPBF. This is because thermal gradients in the melt-pools and remelting of previous layers may destroy the primary nuclei before they can grow to become equiaxed grains [7]. Additionally, the process parameter optimization procedure for obtaining CET is considerably sensitive to the component geometry being build. This implies that several iterations of LPBF fabrication, which is energy and cost intensive, are required before a component with the desired microstructure can be obtained. Similarly, while the eutectic solidification in Al-Si and Al-Ce alloys enhances printability, the mechanical properties of the obtained builds are far inferior to that of precipitation hardened Al alloys produced by conventional means. There is also a possibility of designing Al alloys, where both heterogeneous nucleation in the initial stage of solidification and eutectic solidification at the terminal stage can be synergized [7]. The motivation behind this is to exploit the favourable effects of grain refinement, i.e., trigger CET, during the initial stages of solidification; facilitate effective pore filling by liquid metal in the terminal stage of solidification [18, 20-21]. In this regard computational approaches that estimate the solidified volume fraction of melt pool as a function of temperature could be a useful tool to supplement alloy design of Al alloys with enhanced printability. The example of one such computational study to implement this idea is as follows [7, 20,22].

Fig.1 (a) is a schematic illustration of three stages of solidification in Al alloys. In stage 1, dendrites nucleate. Since the volume fraction of dendrites is initially minimal in the melt, they tend to be in a dangled state and as a result the flow of liquid into the intricate areas for obviating cracking is easily done. In stage 2, the proliferation of dendrites leads to formation of a continuous coherent network and therefore the liquid feeding into complex channels becomes increasingly difficult. Finally, stage 3 solidification is reckoned when the volume fraction of solidified melt approaches ~0.9. At this stage, grains evolve, and their connectivity is gradually established. However, on account of the thermal strains imposed due to rapid solidification conditions, the grains connectivity may be disrupted

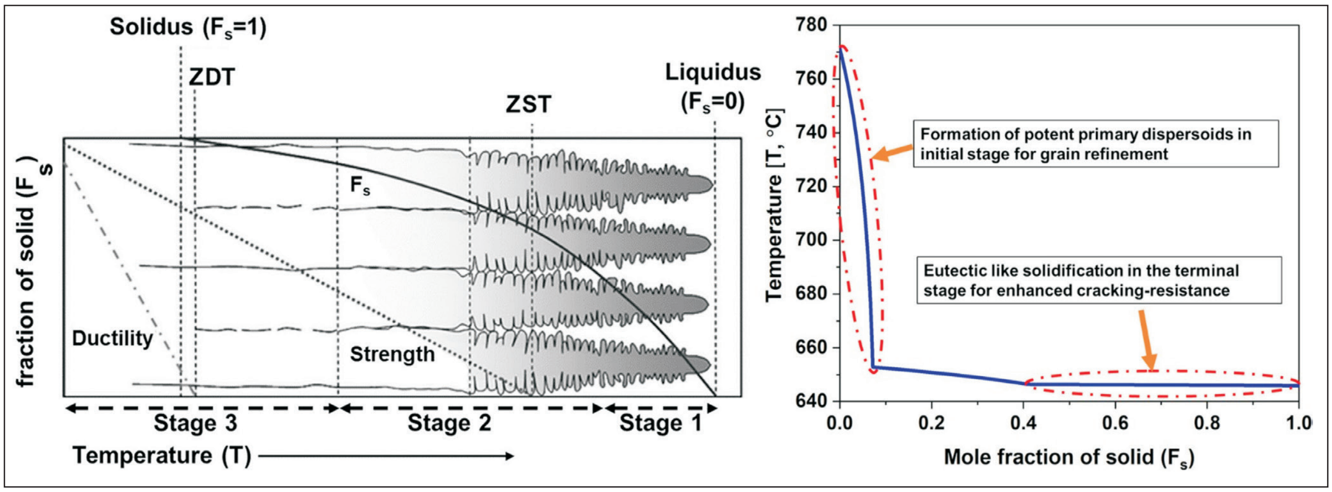

Fig. 1 : (a) Schematic illustrating the dendritic solidification through temperature (T) – fraction of solid (F_s) plot and b) strategy to enhance printability of Al alloys through computational approaches that predict T- F_s curve. Reproduced with permission from Elsevier [7] under Creative Commons Attribution license 4.0 (CC BY-NC-ND)

at isolated regions, leading to entrapment of liquid at intergranular regions. This hinders feeding the liquid deficient regions and results in hot cracking. It was noted that the susceptibility of hot cracking of an Al alloy during solidification are severe during stage 2 and stage 3 of solidification as dendrites obstruct the flow of liquid into intricate cavities. Hence a knowledge of solidified fraction of the melt with respect to temperature can provide important clues to mitigate hot cracking.

With the advent of computational approaches, precise estimation of solidified volume fraction (F_s) of the dendrites in the melt pool can be estimated over the entire temperature (T) range. Various metrics like hot cracking susceptibility index (HCI), critical temperature range (ΔT_{CR}) and freezing range that establish a mathematical functional relationship between T and Fs are devised. These provide an analytical basis for the assessment of printability vis-à-vis alloy composition. This computational pursuit is ideal in assessing the appropriate alloying elements that synergistically maximize the heterogeneous nucleation during initial stages of solidification and promote eutectic solidification during final stage of solidification. For instance, in a typical T-F_s curve (see Fig. 1 (b)), the slope of temperature difference versus solidification fraction (when $F_s < 0.1$) is a measure of nucleation potential. The steeper the initial slope of the T-F_s curve, the larger the domain of constitutional supercooling and subsequent primary nuclei density in the melt pool. On the contrary, in the final stages of solidification, dramatic changes in thermal stresses due to steeper gradients will lead to dissociation of grains and augment hot cracking. Hence, the ideal alloy composition, in terms of printability, is that which exhibits an "L-shaped" T-F_s curve (see Fig.1 (b)). Mishra and Thapliyal [7] simulated the T-F_s curves for 3 Al alloy compositions, namely Al-Ce-Mn, Al-Si-Mg and Al-Mg-Sc-Zr, in Fig. 2. They observed that Al-Ce-Mn alloy exhibits the best printability due to its zero-temperature freezing range and (ΔTCR) during the terminal stage of solidification coupled with eutectic solidification persisting until the solidification of melt pool is complete.

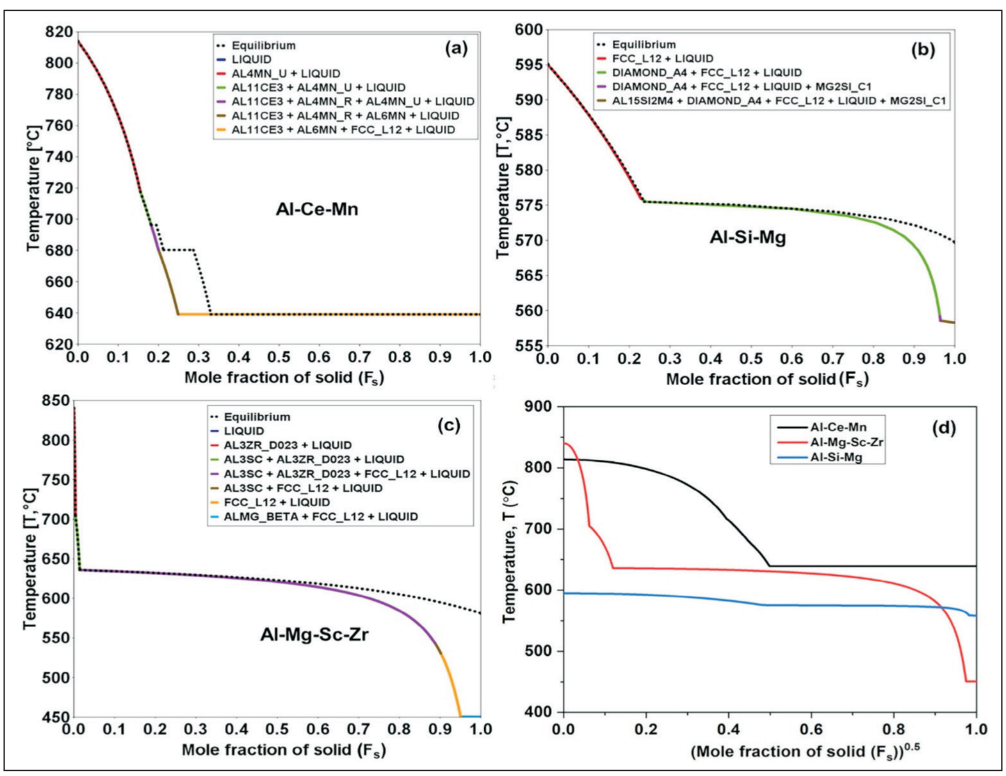

Fig. 2 : T-F_s curves for various alloy systems generated through Schiel — Gulliver Solidification modelling. Reproduced with permission from Elsevier under Creative Commons Attribution license 4.0 (CC BY-NC-ND)

3. Defects and anomalies in LPBF processed Al alloys

Defects generated during LPBF processing of Al alloys are attributed to the powder used and the process parameters employed. The chemistry, morphology and packing ability of powder particles will have a significant influence on the build quality [23]. Powder feedstock employed in LPBF is manufactured through various techniques like gas atomization, plasma rotating electrode process, wire atomization and plasma atomization. The quality of powder stock, specifically its particle size distribution, depends on the processing technique employed. Powders manufactured through gas atomization are widely preferred in industry compared to other methods because this method produces fine spherical powders at an optimal cost [24]. Gas atomization process involves three sequential steps: a) melting of ingots in an inert atmosphere b) atomization of liquid metal in a chamber under the influence of high-pressure gas c) subsequent solidification of atomized powders. Since the gas has lower heat capacity (compared to other cheaper atomization medium, water) the solidification time for a metal droplet is higher and results in generation of powder particles with greater sphericity. Besides sphericity, the flowability and spreadability of Al alloy metal powders on the build substrate also influences the generation of defects during layer-by-layer fabrication [23]. Another major source of defects in Al alloy powders are surface contaminants. For instance, the protective oxide layer that forms on top of the alloy powders mixes with the deposited metal and hampers the quality of the build component by decreasing its wettability w.r.t. the substrate. Furthermore, the presence of oxide in the melt pool alters its surface tension and activates Marangoni flow, which in turn facilitates the formation of keyhole porosity in the build. Oxide contamination in Al powders also affects laser infiltration in the melt pool and results in lack-of-fusion (LOF) defects in the build. Keyhole porosities and LOF defects are more commonly attributed to inadequate process parameter optimization and will be discussed next.

Process parameter related defects in LPBF are mainly categorized as balling, LOF porosity, gas porosity and keyhole porosity [25]. These defects not only depend on laser beam parameters like power, scan velocity, spot diameter of laser beam but also on thermophysical characteristics of the powder, such as its absorptivity and reflectivity. Additionally, powder bed variables, such as hatch spacing and layer thickness, also have an influence on the presence of these defects. Balling is defined as the irregular variation in the melt track height along the deposited direction. Although balling phenomenon is known to occur due to flow instability in the melt pools, the influence of alloy chemistry and purging gas cannot be ruled out. LOF porosity is primarily attributed to lack of overlap between successive melt pool layers owing to insufficient energy input in the bed. LOF porosity is aggravated by turbulent flow in the melt pool, pressure generated due to inert gas flow, ejection of spatter due to boiling of metal pool underneath the laser beam that creates a vapor plume. If inappropriate hatch distances are employed during laser scanning, it will result in creation of rugged concave surfaces that intensify the wetting of subsequently deposited layers to the LOF and increase the size of LOF. Similarly, LOF is also caused by the rise in melting point of powder particles either due to oxide formation on the powder or vast difference in melting points of the constituent elements of an alloy. Keyhole porosities occur when the laser power exceeds a certain threshold and induces instantaneous evaporation of the metal within the melt pool. The subsequent recoil pressure of the gas in its vicinity emits a microjet of pores within a melt pool. The consequent impact of this microjet of pores on the melt pool walls results in spontaneous dissociation of pores and the energy released in this process generates intense acoustic waves that triggers expansion of melt pool into a long, narrow keyhole shaped melt pool. During subsequent laser energy interactions, the acoustic wave generation is further amplified and stable emission of pores into the solidification front occurs. Finally, gas porosities or metallurgical pores form in the build when the gas dissolved in the metal powders during atomization processes get entrapped in the build during solidification. Besides gas pores, all other pores can be controlled or eliminated by carefully optimizing the process parameters in LPBF.

However, optimizing LPBF processing parameters with the intention of minimizing defects in Al alloys, particularly the precipitation hardenable grades, is particularly challenging owing to the additional requirement of preventing hot cracking in them (see section 2). The different factors that lead to the formation of defects in Al alloys are as follows. Certain grades of Al alloys (eg. 5xxx, 6xxx and 7xxx series alloys) contain volatile elements like Mg and Zn that evaporate when the energy input is high [26], which causes turbulence in the melt pools. Turbulence in the melt pool leads to balling and also deteriorates the surface finish of the build. In addition, the high reflectivity of laser on Al reduces the energy input and is responsible for the presence of LOF porosity in the builds. Fig.3 schematically illustrates various LOF defects in Al alloys.

Keyhole pores are more likely to be formed at laser track turning regions, where longer scan duration results in profound heat accumulation. However, they can also form when the rear keyhole wall undergoes breakdown in the transient melting regime. During re-entry scan when the energy density reverts to steady state, surface tension overcomes the recoil pressure and results in destruction of keyhole and resultant entrapment of pores into the melt pool. The dynamic impact of spatter particles with keyhole also causes keyhole instability. Therefore, a higher degree of spatter can also increase the number of keyhole porosities.

Gas pores in Al alloys are introduced into the melt pool either due to the presence of moisture on the substrate or any hydrocarbon adhered onto powder surface. Unlike LOF pores they are small (< 50 μm) and have a near spherical shape. Hydrogen induced porosity is prevalent in Al alloys since hydrogen is soluble in liquid Al melt but has an order of magnitude lower solubility in solid Al. Furthermore, melt pool surface instabilities that manifest due to turbulence in the melt pool will generate momentary protrusion and disintegration of melt surface to create passageways for gas entrapment. Similarly, spatter also contributes to confinement of gas in the time interval between spatter ejection and its reintegration into the melt pool.

It was also observed that the spatial distribution of pores in the build layers is heterogeneous. This is attributed to migration of the generated pores under the combined forces of Marangoni convection, which manifests due to gradients in surface tension, thermocapillary forces and buoyant forces in the melt pool. Depending on the oxide contamination in the powders, the pores experience a centripetal drag force or centrifugal force. All these factors lead to irregularities in spatial pore distribution and result in vast variation of the mechanical properties. The mitigation of all these defects during LPBF processing of Al alloys is an active area of research. Currently two broad strategies are adopted to mitigate porosity for LPBF'ed Al alloys. First one involves establishing the process map between printing parameters (laser power, scan speed, hatch distance and layer thickness) and volume of fraction porosity obtained. Complemented with state-of-the-art tools like X ray tomography, an indirect correlation of pore spatial distribution and their morphology with printing parameters can be ascertained on post-mortem basis [32, 33].

Secondly with further advances in *in situ* X-ray imaging, real time analysis of formation of pore formation and their propagation has been uncovered. It was shown that for AlSi10Mg alloy, the pore motion is manifested due to the inherent competition between thermocapillary force (induced by spatial thermal gradients) and the drag force induced by melt pool. If the laser parameters are tuned such that thermocapillary force dominates drag force, the pores can be effectively eliminated [34]. However, the magnitude of thermocapillary forces is found to be spatially heterogeneous. Near the axis of laser beam, the pores escape into the depression zone and are therefore effectively eliminated. However, the farther from laser beam axis, the pores either form a circulation motion within the pool or undergo erratic movements. Therefore, a thorough understanding of how laser process parameters affect spatial thermocapillary force can provide robust insights for controlling porosity. Qu et al. [35,36] have further shown that incorporation of TiC nanoparticles, has remarkable effect on melt flow behavior. Here again, *in situ* X-ray imaging revealed, TiC nanoparticle interaction lead to following changes for LPBF'ed AA6061 alloy: a) enhancement in melt pool viscosity decreases the turbulent fluctuations in melt pool both in conduction and keyhole melting modes b) improved surface roughness. Hence incorporation of nanoparticles in the melt and *in situ* X-ray imaging of melt pool surface evolution has vast potential to further tailor surface roughness and porosities in LPBF of Al alloys.

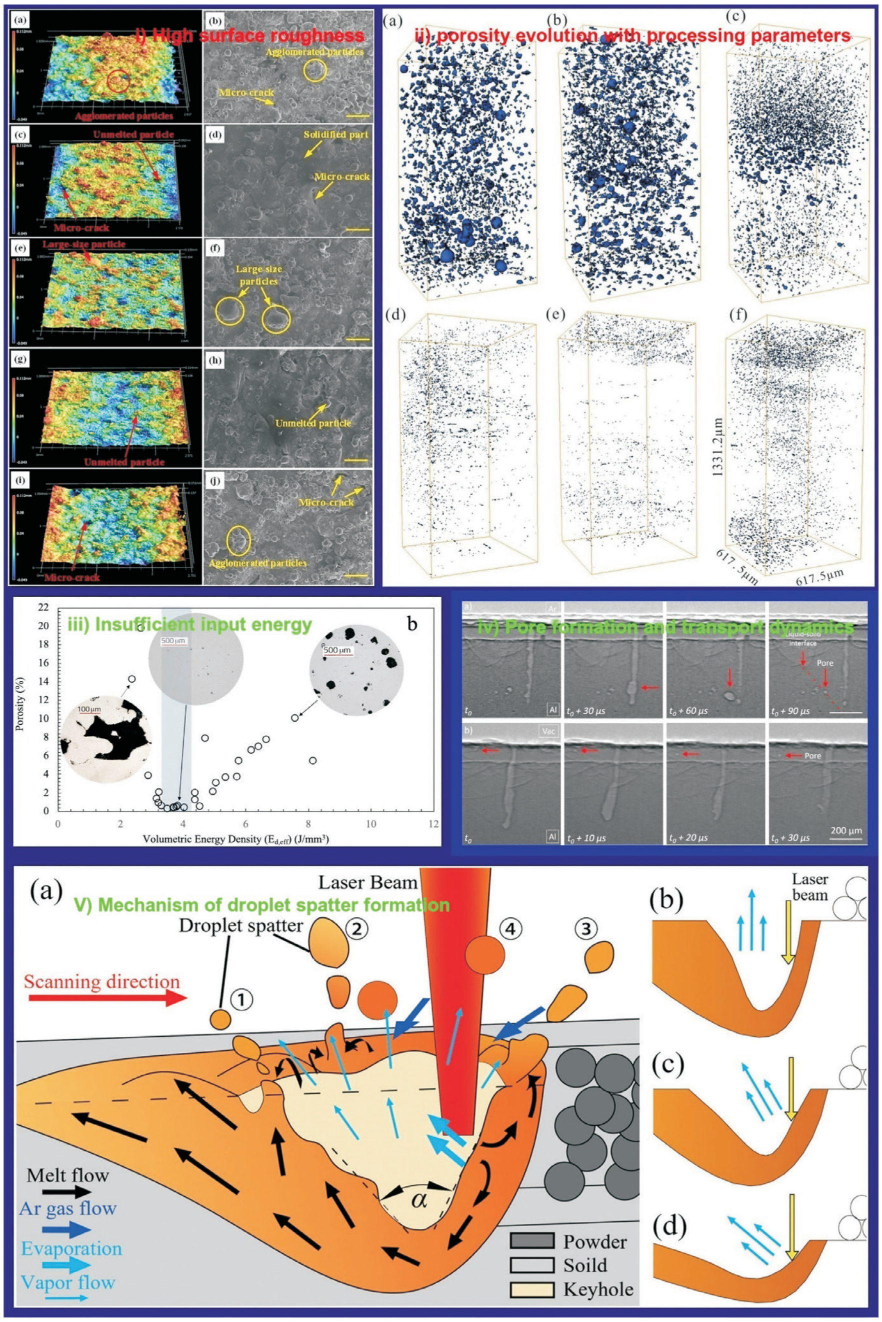

Fig. 3 : Schematic depicting lack of fusion defect generation in LPBF due to factors like (i) Topography and morphology of AlSi10Mg extracted from various surfaces of different curvatures [27] (ii) 3D distribution of micropores in as built, post process heat treated, post deposition rolling at various loads for Al-Cu6.3 alloy[28] (iii) porosity generation due to insufficient power [29] (iv) pore formation and transport dynamics [30] (v) Formation mechanism of droplet spatter at various input energies [31] Reproduced with permission from Elsevier under Creative Commons Attribution license 4.0

4. Heat treatments/post processing effects on microstructural and defect evolution of Al alloys

Table 1 lists the Al alloys fabricated via LPBF either for commercial or research interests [37]. A vast chunk of LPBF investigations were undertaken on Al-Si-(Mg) as these alloys undergo eutectic solidification and offer nominal resistance to hot cracking. While these alloys possess a maximum yield strength of ~300 MPa LPBF'ed high strength Al-Cu based alloys achieved yield strengths (~125 to 525 MPa). Such broad range of yield strength values in Al-Cu based alloys vis-à-vis Al-Si based alloys is attributed to diverse heat treatments imparted and the complexities in their alloy chemistry. Therefore, LPBF as a processing methodology for Al alloys is generally a trade-off between printability and optimum mechanical properties.

Table 1. Al alloys developed by LPBF and their composition [37]

Series /Designation	Al Alloy	Composition (wt.%)
1xxx	AA1050	-----
2xxx	AA2017	Cu (3.5–4.5), Mg (0.4–1), Si (0.2–0.8)
	AA2024	Cu (3.8–4.9), Mg (1.2–1.8), Mn (0.3–0.9)
	AA2219	Cu (5.8–6.8), Mn (0.2–0.4)
	AA2618	Cu (1.8–2.7), Mg (1.2–1.8), Ni (0.8–1.4)
5xxx	AA5083	Mg (4–4.9), Mn (0.4–1)
	AA5356	Mg (4.5–5.5)
6xxx	AA6061	Mg (0.8–1.2), Si (0.4–0.8), Cu (0.15–0.4)
7xxx	AA7020	Zn (4–5), Mg (1–1.4)
	AA7050	Zn (5.7–6.7), Cu (2–2.6), Mg (1.9–2.6)
	AA7075	Zn (5.1–6.1), Mg (2.1–2.9), Cu (1.2–2)
Al-Si	AlSi5Cu3Mg	Si (4.5–6), Cu (2.6–3.6), Mg (0.15–0.45)
	AlSi7Mg0.3	Si (6.5–7.5), Mg (0.25–0.45)
	AlSi7Mg0.6	Si (6.5–7.5), Mg (0.45–0.7)
	AlSi9Cu3	Si (8–11), Cu (2–4)
	AlSi10Mg	Si (9–11), Mg (0.2–0.45)
	AlSi12	Si (11–13)
	AlSi20	Si (18–22)
	AlSi50	Si (47–53)
Al-Mg-Sc	Scalmalloy®	Mg (4–4.9), Sc (0.6–0.8)

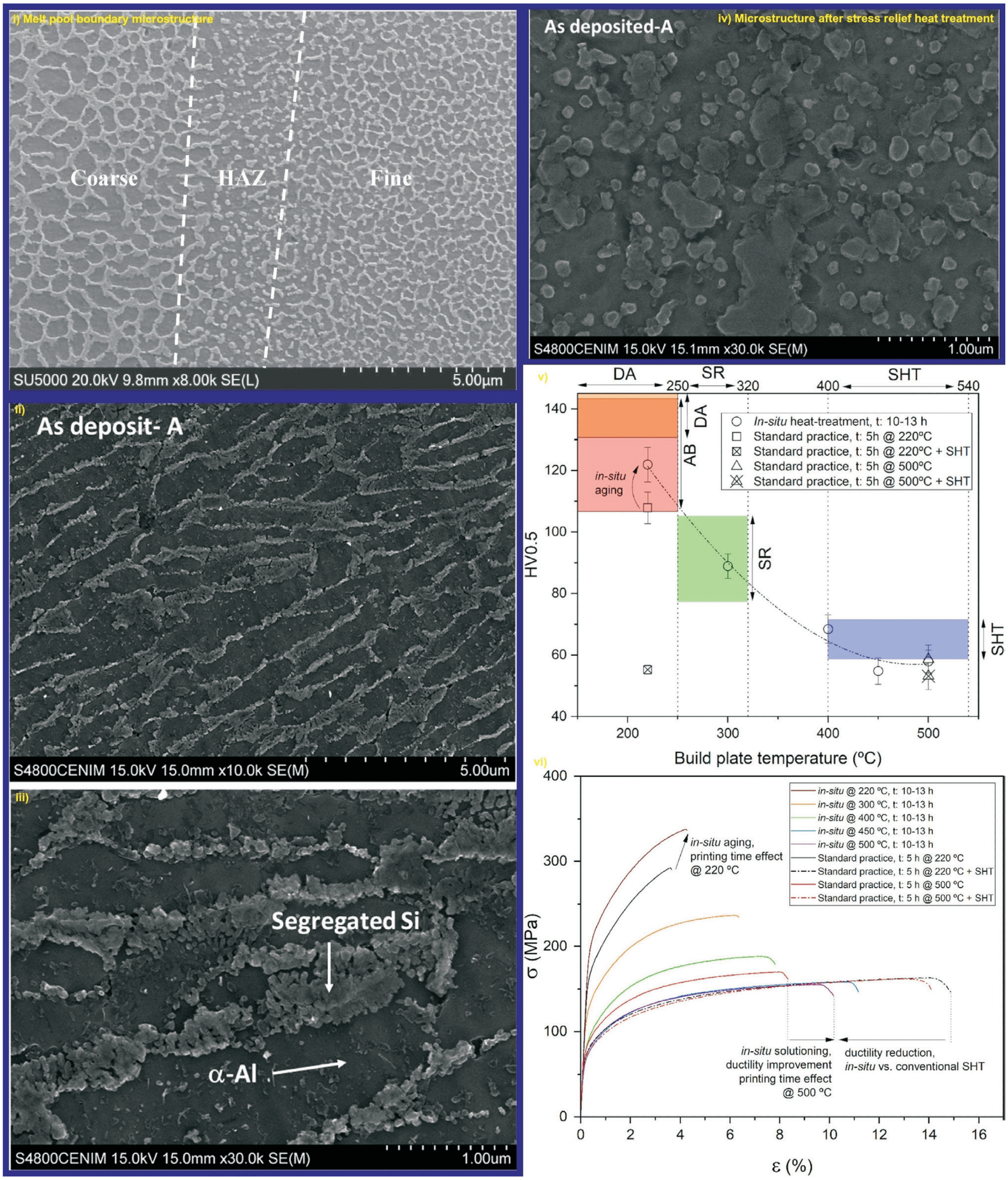

Fig. 4: i) Melt pool morphology of AlSi10Mg alloy depicting HAZ [38] ii) and iii) depicting the as built eutectic microstructure in further detail and iv) evolution of microstructure with stress relief heat treatment at 573 K for 2 hours [39] v) Effect of heat treatment on microhardness and vi) Effect of heat treatment on tensile properties [40]. Reproduced with permission from Elsevier under Creative Commons Attribution license 4.0

For heat treatable alloys (2xxx, 6xxx and 7xxx) manufactured by LPBF, precipitation hardening is typically achieved through formation of Al_2Cu, Al_2CuMg, $MgZn_2$ precipitates. In general, the heat treatments cycles employed for LPBF'ed Al alloys are stress relief annealing (200-400°C), homogenization at 480 – 540°C to uniformly distribute precipitates, and solution treatment followed by quenching to retain solid solution hardening elements (up to the solidus temperature of alloy) and aging (115-190°C) for up to 48 hours [41]. Though there are various temper designations based on sequence of heat treatments for cast and wrought alloys, the tempers that do not involve cold work are employed for heat treatment of LPBF processed Al alloys. Fig 4 (a) displays a typical microstructure comprising heat affected zone (HAZ) for a LPBF processed AlSi10Mg alloy in the as built condition. Fig. 4 (b) and (c) depicts the typical eutectic microstructure encountered in these materials. Though not depicted here, the overlapping multipool morphology is representative of a broad spectrum of Al alloys. From Fig.4 (a), it is evident that the as built microstructure (AlSi10Mg) is inhomogeneous, i.e., it has fine microstructural features at the middle of melt pools and coarser features at melt pool boundaries [37]. This is ascribed to spatially heterogeneous thermal gradients. The appearance of coarser features at melt pool boundaries has been shown to be generic across different LPBF processed Al alloys. Fig. 4d illustrates the microstructure in stress relief heat treatment condition. Here, the eutectic microstructure is dismantled, and Si particles evolve and gradually coarsen with increase in temperature (Fig.4 (d)) [41]. Generally, the heat treatment protocols are tailored with respect to the alloy chemistry and the resultant mechanical properties are sensitive to the heat treatments employed, as depicted in Figs 4e and (f).

Besides AlSi10Mg alloys, heat treatment studies were performed on Al-Cu and Al-Zn-Mg alloys. Since precipitation hardened 2xxx, 6xxx and 7xxx series alloys have printability issues due to hot cracking, these alloys are printed either through incorporation of ex situ inoculants (like TiB_2 or SiC) or by incorporating eutectic forming elements like Si in the alloy. However, the precipitation sequence of LPBF processed Al alloys is different than their conventionally manufactured counterparts, when subjected to the same heat treatment. For instance, the addition of Si triggers eutectic microstructure formation in these alloys during ageing. The possible reasons for such peculiar phase evolution on heat treatment could be ascribed to the fact that LPBF processing involves non-equilibrium cooling that extends its solid solution capabilities, introduces tensile residual stresses, imparts a columnar microstructure and facilitates *in-situ* phase transformations during repeated laser scans. Moreover, LPBF processing can vaporize volatile elements like Zn from the powders, which also has a significant influence on the response of the final build to heat treatment.

With the aid of computational alloy design approaches, Al alloys that have both excellent printability and remarkable mechanical properties obtained through heat treatments have been designed [17]. Two different strategies are presently pursued in such approaches. First, both Sc and Zr are added as microalloying elements, which form primary micron scale $L1_2$ precipitates when the alloy powders are melted. These precipitates help in grain refinement and CET during solidification. Further, subsequent heat treatment precipitates secondary $L1_2$ nano-precipitates. These nano-precipitates prevent grain coarsening and facilitate precipitation hardening in the alloy. In the second strategy, non-reactive ceramic dispersoids are added in some heat-treatable Al alloy (eg. 6xxx, 2xxx or 7xxx series alloys) and developed into powders [17]. The ceramic dispersoids perform a similar function as that of Al-Sc and Al-Zr precipitates in the Al-Sc-Zr alloys in terms of arresting grain growth and providing particulate strengthening. Additionally, the strength of the alloy can be enhanced by choosing the appropriate age hardening heat treatment, which can optimize the volume fraction, coherency and size of the precipitates. Among these two different strategies, the former is usually preferred as they have refined microstructures and remarkably high yield strengths (~ up to 570 MPa) when they are subjected to ageing treatments at 300-325°C for 4-5 hours. While the addition of ceramic dispersoids is reasonably successful, these composites are expected to have poor fatigue life [17].

Apart from microstructural modifications, the role of heat treatments in altering the porosity of Al alloys has been explored through X-ray tomography measurements of pore spatial location, and morphology. Various heat treatments were found to enhance porosity compared to as built condition [41,42]. The enhancement in porosity is ascribed to destruction of eutectic Si network, its subsequent transformation into large spherical particles, growth in size of both large and small pores for AlSi10Mg [42]. However, despite increase in porosity, AlSi10Mg alloys exhibited enhanced fatigue resistance from post processed heat treatments. Bagherifard et al. [43] attributed the improved fatigue response to microstructural homogeneity, minimization of residual stress and increment in ductility caused by T6 heat treatment. However, it is difficult to generalize such increased damage tolerance to other Al alloys and further studies are required to ascertain the role of post process heat treatments on porosity-microstructure and fatigue correlations for LPBF processed precipitation hardened Al alloys.

In summary, for Al alloys that have eutectic microstructures, such as Al-Si based alloys, the post heat treatment microstructures are dependent on the specific heat treatment applied. Solution treatment, followed by ageing and high temperature annealing dismantles the eutectic network. Alternately, while ageing followed by low temperature heat treatment will render the eutectic microstructure intact, T6 temper treatment leads to the evolution of fine Si precipitates. In contrast, for 2xxx, 6xxx and 7xxx series alloys, direct ageing results in optimal mechanical properties. However, there is a great potential to redefine heat treatment protocols for LPBF processed Al alloys considering that they are fabricated under non-equilibrium solidification conditions, which leads to supersaturation of constituents in the Al matrix.

5. Fatigue response of LPBF processed Al alloys

Fig.5 shows the Ashby plot depicting the strength versus ductility for Al alloys processed by different methods. As can be seen clearly, all LPBF processed Al alloys surpass conventionally manufactured precipitation hardened alloys in terms of strength. In some cases, the ductility of LPBF alloys is also significantly better than that of its conventionally manufactured counterparts. However, LPBF

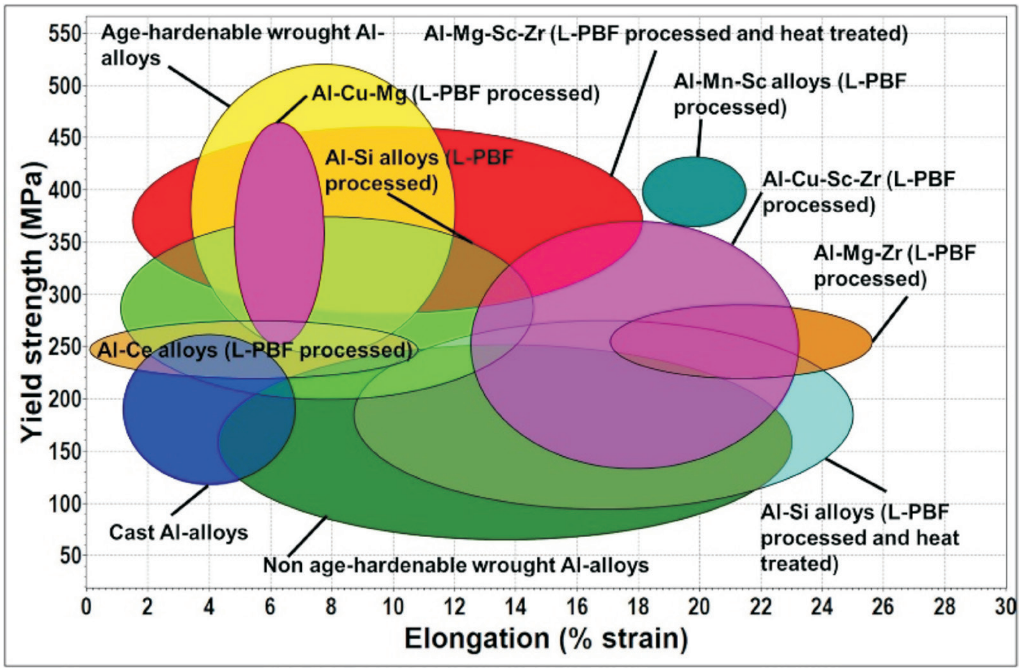

Fig. 5 : Ashby plot depicting the room temperature tensile yield strength and elongation of Al alloys [7]. Reproduced with permission from Elsevier under Creative Commons Attribution license 4.0 (CC BY-NC-ND)

processed Al-Sc-Zr alloys underperform in fatigue loading vis-à-vis their conventionally manufactured counterparts. Fatigue endurance limit (FEL) of LPBF'ed Sc and Zr containing alloys subjected to either ageing or hot isostatic pressing (HIP) treatments is ~100 MPa compared to 160 MPa achieved for wrought AA5083 and AA7075 alloys. On the contrary AlSi10Mg alloys, which have good printability, also has a FEL of ~ 125 MPa in the T6 temper condition. However, the FEL/UTS ratio of Al-Si based alloys is ~0.43, which is significantly higher compared to that of Al-Sc-Zr alloys (~0.19). It must however be noted that Al-Si alloys exhibit a wide variation in FEL and depends on the spatial extent of eutectic microstructure and the presence of inter-dendritic Si phase at the boundaries of melt pool. This Si network leads to crack deflection and delays fatigue fracture. Therefore, heat treatments that destroy this Si network deteriorates the FEL of Al-Si alloys.

Similarly, the FEL of LPBF processed precipitation strengthened alloys is significantly lower compared to their conventionally manufactured counterparts. This is however attributed to the presence of defects in the former, which in turn is ascribed to their poor printability. In these alloys, fatigue cracks originate microscopically at regions of high residual stresses, delaminated built layers, rough surfaces, LOF porosity, unmelted powder particles, and surface cracks [44-46].

In addition, microstructural features like internal pores and cracks, columnar grains, oxide inclusions and regions with microsegregation are also sources for fatigue crack initiation. Hence, unlike conventional metallic alloys where localized plastic deformation at microscopic regions and grain boundaries initiate fatigue cracks, presence of multiple crack initiators in LPBF processed alloys aggravate fatigue crack nucleation and its subsequent growth. In engineering materials, the nucleation of fatigue crack consumes up to ~20 % of the fatigue life. Evidently, the nucleation of fatigue crack happens even at lower threshold in defect prone materials. As the formation of defects is inevitable in LPBF of Al alloys, the ideal strategy to enhance FEL must be based on damage tolerant assessment approaches. Hence, a thorough understanding of fatigue crack propagation dynamics based on fracture mechanics approaches holds the key to augment fatigue life.

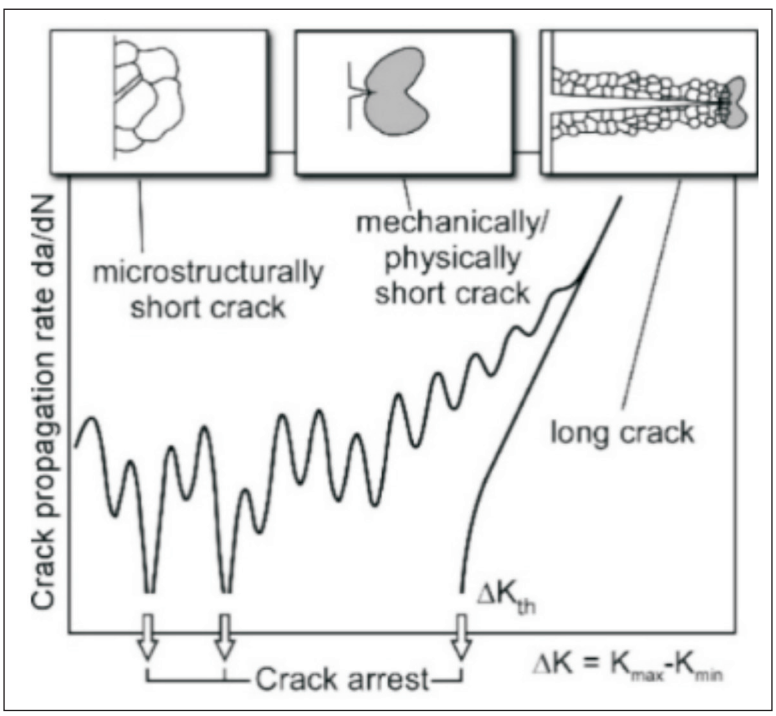

Fig. 6 : A schematic illustration of proliferation of fatigue cracks in engineering materials [47]. Reproduced with permission from Elsevier under Creative Commons Attribution license 4.0

Fig. 6 illustrates the evolution of fatigue crack with increment in loading cycles. In the microcracking regime, crack propagation rate fluctuates due to its interaction with microstructural features. The inherent fatigue limit is characterized by stress threshold at which the arrest of a significant crack among the larger number of cracks happens and is an important parameter that influences high cycle fatigue life. A material where the largest possible crack is arrested for a particular fatigue threshold is considered desirable. Once the micro crack crosses the fatigue threshold, it becomes a short crack and extends up to the size of a plastic zone. Further transition to long crack regime is reckoned when crack closure phenomenon attains invariance with regard to crack depth. From this stage, accelerated crack growth ensues and finally leads to fracture. Fatigue crack growth orientation is complicated in the presence of notches which amplify stress gradients and promote a multitude of crack closure mechanisms. In typical service conditions, where multi axial loads are encountered, fatigue cracks grow under mixed mode. Fatigue crack orientation of AM specimens under different loading conditions is shown to align in the direction of maximum principal stress indicating that an inherently brittle failure mechanism is operative [48]. Though crack arrest in microcrack regime (due to its interaction with microstructural attributes) and crack closure (due to notch effects) govern fatigue limit, the former mainly influences the fatigue life. Hence the optimum strategy to improve fatigue life of LPBF Al alloys is to tailor processing conditions that tailor the micro and mesostructural features. To achieve this goal, the role of processing conditions in defect size distribution, morphology and their spatial distributed to be precisely characterized and linked to fracture mechanics-based approaches.

Concluding remarks

To summarize, the initial strategies to enhance the printability of Al alloys are based on two approaches: a) grain refinement approach through alloying with Sc, Zr, Hf, Ti, V. It results in the formation of coherent nano-precipitates with Al matrix, promote heterogeneous nucleation and CET b) eutectic solidification approach in which alloying elements that favour eutectic formation will allow effective filling of pores. State of art computational alloy design techniques aim to synergize both these approaches through assessment of temperature-solidification fraction curves for diverse Al alloy compositions. As a result, the alloys that promote large constitutional supercooling during initial stage of solidification and eutectic solidification at the terminal stage have good printability.

The origin of defects and pores during LPBF of Al alloys are either ascribed to inherent defects in powder feed stock or process parameters driven anomalies. The conventional method of defect mitigation is through post-mortem quantification of spatial location and morphology of defects with tools like X-ray tomography and mapping them with laser process parameters. As a result, optimized laser process parameters that maximize component density are chosen. The recent advent of *in-situ* X-ray imaging provided new insights into pore formation and their evolution. If a melt pool is dominated by drag force, it will maximize pore formation while a melt pool dominated by thermocapillary force will eliminate pores. Likewise, incorporation of nanoparticles will create stable melt pool and minimize surface roughness of final part since the former increases the viscosity of the melt. Further studies are required to ascertain how nanoparticles affect viscosity of the alloys designed through computational approaches mentioned above.

The stability of eutectic microstructure forming LPBF'ed Al alloys are very sensitive to post process heat treatments. Likewise, heat treatment of LPBF'ed precipitation hardening Al alloys will result in complex phase transformations vis-à-vis their conventionally manufactured counterparts. The possible reasons for such peculiar phase evolution on heat treatment could be ascribed to the fact that LPBF processing involves non-equilibrium cooling that extends its solid solution capabilities, introduces tensile residual stresses, imparts a columnar microstructure and facilitates *in-situ* phase transformations during repeated laser scans. Alloying elements like Sc and Zr are very effective in promoting CET during primary solidification and facilitating formation of secondary $L1_2$ precipitates during post process heat treatments. In Al alloys, post process heat treatments enhance porosity but increase fatigue life. Despite reduction in strength due to porosity, the improved fatigue response is attributed to microstructural homogeneity, minimization of residual stress and increment in ductility as a result of heat treatment.

Since fatigue cracks originate microscopically at regions of high residual stresses, delaminated built layers, rough surfaces, LOF porosity, unmelted powder particles, and surface cracks, LPBF'ed Al alloys have lower FEL compared to conventionally manufactured alloys. As nucleation of fatigue crack happens even at lower threshold in these defect prone materials, the key to enhancing fatigue life is based on damage tolerant assessment approaches. Fatigue crack orientation of AM specimens under different loading conditions is shown to align in the direction of maximum principal stress indicating that an inherently brittle failure mechanism is operative. Engineered micro and mesostructural features that are aimed at enhancing fatigue threshold are desired for increasing fatigue life.

References

[1] E. Georgantzia, M. Gkantou, G.S. Kamaris, Aluminium alloys as structural material: A review of research, ***Eng. Struct***. 227 **(2021)** 111372. https://doi.org/10.1016/j.engstruct.2020.111372

[2] J.L. Cann, A. De Luca, D.C. Dunand, D. Dye, D.B. Miracle, H.S. Oh, E.A. Olivetti, T.M. Pollock, W.J. Poole, R. Yang, C.C. Tasan, Sustainability through alloy design, ***Prog. Mater. Sci.*** 117 **(2021)** 100722. https://doi.org/10.1016/j.pmatsci.2020.100722

[3] M. Glazoff, V. Zolotorevsky, N. Belov, ***Casting Aluminium alloys***, 1st edition, Elsevier, **2007**.

[4] D. Raabe, C.C. Tasan, E.A. Olivetti, Strategies for improving sustainability of structural materials, ***Nature,*** 575 **(2019)** 64. https://doi.org/10.1038/s41586-019-1702-5

[5] N.T. Aboulkhair, M. Simonelli, L. Parry, I. Ashcroft, C. Tuck, R. Hague, 3D printing of Aluminium alloys: Additive Manufacturing of Aluminum alloys using selective laser melting, ***Prog. Mater. Sci***. 106 **(2019)** 100578. https://doi.org/10.1016/j.pmatsci.2019.100578

[6] H.R. Kotadia, G. Gibbons, A. Das, P.D. Howes, A review of laser powder fusion additive manufacturing of aluminium alloys: microstructure and properties, ***Addit. Manuf.*** 46 **(2021)** 102155. https://doi.org/10.1016/j.addma.2021.102155

[7] R.S. Mishra, S. Thapliyal, Design approaches for printability-performance synergy in Al alloys for laser powder bed additive manufacturing, ***Mater. Des.*** 204 **(2021)** 109640. https://doi.org/10.1016/j.matdes.2021.109640

[8] P.A. Rometsch, Y. Zhu, X. Wu, A. Huang, Review of high strength aluminium alloys for additive manufacturing by laser powder bed fusion, ***Mater. Des.*** 219 **(2022)** 110779. https://doi.org/10.1016/j.matdes.2022.110779

[9] A.T. Clare, R.S. Mishra, M. Merklein, H. Tan, I. Todd, L. Chechik, J. Li, M. Bambach, Alloy design and adaptation for additive manufacture, ***J. Mater. Process. Tech.*** 299 **(2022)** 117358. https://doi.org/10.1016/j.jmatprotec.2021.117358

[10] A. Martucci, A. Aversa, M. Lombardi, Ongoing challenges of laser powder bed fusion processing of Al alloys and potential solutions from literature: A review, ***Materials.*** 16 **(2023)** 1084. https://doi.org/10.3390/ma16031084

[11] I.M. Kusoglu, B. G'kce, S. Barcikowski, Research trends in laser powder bed fusion of Al alloys within the last decade, ***Addit. Manuf.*** 36 **(2020)** 101489. https://doi.org/10.1016/j.addma.2020.101489

[12] J.H. Martin, B.D. Yahata, J.M. Hundley, J.A. Mayer, T.A. Schaedler, T.M. Pollock, 3D printing of high strength aluminium alloys, ***Nature,*** 549 **(2017)** 365 https://doi.org/10.1038/nature23894

[13] A. De Luca, D.C. Dunand, D.N. Seidman, Microstructure and mechanical properties of a precipitation strengthened Al-Zr-Sc-Er-Si alloy with very small Si content, ***Acta Mater.*** 144 **(2018)** 80. https://doi.org/10.1016/j.actamat.2017.10.040

[14] J. A. Glerum, C. Kenel, T. Sun, D.C. Dunand, Synthesis of precipitation strengthened Al-Sc, Al-Zr and Al-Sc-Zr alloys via selective laser melting of elemental powder blends, ***Addit. Manuf.*** 36 **(2020)** 101461. https://doi.org/10.1016/j.addma.2020.101461

[15] Z. Fan, F. Gao, Y. Wang, H. Men, L. Zhao, Effect of solutes on grain refinement, ***Prog. Mater. Sci.*** 123 **(2022)** 100809. https://doi.org/10.1016/j.pmatsci.2021.100809

[16] J. Røyset, N. Ryum, Scandium in aluminium alloys, ***Int. Mater. Rev.*** 50 **(2005)** 19. https://doi.org/10.1179/174328005X14311

[17] R.A. Michi, A. Plotkowski, A. Shyam, R.R. Dehoff, S.S. Babu, Towards high temperature applications of aluminium alloys enabled by additive manufacturing, ***Int. Mater. Rev.*** 67 **(2022)** 298. https://doi.org/10.1080/09506608.2021.1951580

[18] C.N. Ekaputra, D. Weiss, J.E. Mogonye, D.C. Dunand, Eutectic, precipitation strengthened alloy via laser fusion of blends of Al-7Ce-10Mg (wt.%), Zr and Sc powder, ***Acta Mater.*** 246 **(2023)** 118676. https://doi.org/10.1016/j.actamat.2023.118676

[19] J.U. Rakhmonov, N.Q. Vo, J.R. Croteau, J. Dorn, D.C. Dunand, Laser melted Al-3.6Mn-2Fe-1.8Si-0.9Zr (wt.%) alloy with outstanding creep resistance via formation of α -Al(FeMn)Si precipitates, ***Addit. Manuf.*** 60 **(2022)** 103285. https://doi.org/10.1016/j.addma 2022.103285

[20] Z. Yang, C. Chen, D. Li, Y. Wu, Z. Geng, V. Konakov, K. Zhou, An additively manufactured heat resistant Al-Ce-Sc-Zr alloy: Microstructure, mechanical properties and thermal stability, ***Mater. Sci. Eng. A.*** 872 **(2023)** 144965. https://doi.org/10.1016/j.msea.2023.144965

[21] H. Hyer, A. Mehta, K. Graydon, N. Kljestan, M. Knezevic, D. Weiss, B. McWilliams, K. Cho, Y. Sohn, ***Addit. Manuf.*** 52 **(2022)** 102657. https://doi.org/10.1016/j.addma.2022. 102657

[22] S. Thapliyal, M. Komarasamy, S. Shukla, L. Zhou, H. Hyer, S. Park, Y. Sohn, R.S. Mishra, An integrated computational materials engineering anchored closed loop method for design of aluminium alloys for additive manufacturing, ***Materialia,*** 9 **(2020)** 100574. https://doi.org/10.1016/j.mtla.2019.100574

[23] A. Mostafaei, C. Zhao, Y. He, S.R. Ghiaasiaan, Bo. Shi, S. Shao, N. Shamsaei, Z. Wu, N. Kouraytem, T. Sun, J. Pauza, J.V. Gordon, B. Webler, N.D. Parab, M. Asherloo, Q. Guo, L. Chen, A.D. Rollett, Defects and anomalies in powder bed fusion additive manufacturing, ***Curr. Opin. Solid. State. Mater. Sci.*** 26 **(2022)** 100974. https://doi.org/10.1016/j.cossms.2021.100974

[24] K. Kassym, A. Perveen, Atomization process of metal powders for 3D printing, ***Mater. Today Proc.*** 26 **(2020)** 1727. https://doi.org/10.1016/j.matpr.2020.02.364

[25] S. Wang, J. Ning, L. Zhu, Z. Yang, W. Yan, Y. Dun, P. Xue, P. Xu, S. Bose, A. Bandyopadhyay, Role of porosity defects in metal 3D printing: Formation mechanisms, impacts on properties and mitigation strategies, ***Mater. Today.*** 59 **(2022)** 133. https://doi.org/10.1016/j.mattod.2022.08.014

[26] J. Liu, P. Wen, Metal vaporization and its influence during laser powder bed fusion process, ***Mater. Des.*** 215 **(2022)** 110505. https://doi.org/10.1016/j.matdes.2022.110505

[27] Y. Zhou, F. Ning, P. Zhang, A. Sharma, Geometrical, microstructural and mechanical properties of curved surface AlSi10Mg parts fabricated by powder bed fusion additive manufacturing, ***Mater. Des.*** 198 **(2021)** 109360. https://doi.org/10.1016/j.matdes.2020.109360

[28] J. Gu, S. Yang, M. Gao, J. Bai, Y. Zhai, J. Ding, Micropore evolution in additively manufactured aluminium alloy under heat treatment and inter layer rolling, ***Mater. Des.*** 186 **(2020)** 108288. https://doi.org/10.1016/j.matdes.2019.108288

[29] P. Ferro, R. Meneghello, G. Savio, F. Berto, A modified volumetric energy density-based approach for porosity assessment in additive manufacturing process design, ***Int. J. Adv. Manuf. Technol.***110 **(2020)** 1911. https://doi.org/10.1007/s00170-020-05949-9

[30] A.A. Martin, N.P. Calta, J.A. Hammons, S.A. Khairallah, M.H. Nielsen, R.M. Shuttlesworth, N. Sinclair, M.J. Matthews, J.R. Jeffries, T.M. Willey, J.R.I. Lee, Ultrafast dynamics of laser-metal interactions in additive manufacturing alloys captured by *in situ* X-ray imaging, ***Materialstoday. Advances,*** 1 **(2019)** 100002. https://doi.org/10.1016/j.mtadv.2019.01.001

[31] D. Wang, W. Dou, Y. Ou, Y. Yang, C. Tan, Y. Zhang, Characteristics of droplet spatter behavior and process correlated mapping model in laser powder bed fusion, ***J. Mater. Res. Technol.*** 12 **(2021)** 1051. https://doi.org/10.1016/j.jmrt.2021.02.043

[32] P. J. Withers, C. Bouman, S. Carmignato, V. Cnudde, D. Girimaldi, C.K. Hagen, E. Maire, M. Manley, A. Du Plessis, S.R. Stock, X-ray computed tomography, ***Nature Rev. Method Primers.*** 1 **(2021)** 18. https://doi.org/10.1038/s43586-021-00015-4

[33] H. Yang, J. Sha, D. Zhao, F. He, Z. Ma, C. He, C. Shi, N. Zhao, Defect control of aluminium alloys and their composites fabricated via laser powder bed fusion, ***J. Mater. Proc. Tech.*** 319 **(2023)** 118064. https://doi.org/10.1016/j.jmatprotec.2023.118064

[34] S.M.H. Hoojjatzadeh, N.D. Parab, W. Yan, O. Guo, L. Xiong, C. Zhao, M. Qu, L.L. Escano, X. Xiao, K. Fezzaa, W. Everhart, T. Sun, L. Chen, Pore elimination mechanism during 3D printing of metals, ***Nat. Commun.*** 10 **(2019)** 3088. https://doi.org/10.1038/s41467-019-10973-9

[35] M. Qu, Q. Guo, L. I. Escano, J. Yuan, S.M.H. Hoojjatzadeh, S.J. Clark, , K. Fezzaa, T. Sun, L. Chen, Controlling melt flow by nanoparticles to eliminate surface wave induced surface fluctuation, ***Addit. Manuf.*** 59 **(2022)** 103081. https://doi.org/10.1016/j.addma. 2022.103081

[36] M. Qu, Q. Guo, L. I. Escano, A. Nabaa, K. Fezzaa, L. Chen, Nanoparticle enabled increase of energy efficiency during laser metal additive manufacturing, ***Addit. Manuf.*** 60 **(2022)** 103242. https://doi.org/10.1016/j.addma.2022.103242

[37] M. Laleh, E. Sadeghi, R.I. Revilla, Q. Chao, N. Haghdadi, A.E. Hughes, W. Xu, I.D. Graeve, M. Qian, I. Gibson, M.Y. Tan, Heat treatment for metal additive manufacturing, ***Prog. Mater. Sci.*** 133 **(2023)** 101051. https://doi.org/10.1016/j.pmatsci.2022.101051

[38] B. Liu, B.Q. Li, Z. Li, Selective laser remelting of an additive layer manufacturing process on AlSi10Mg, ***Results in Physics,*** 12 **(2019)** 982. https://doi.org/10.1016/j.rinp.2018.12.018

[39] J. de Damborenea, A. Conde, M. Gardon, G.A. Ravi, M. A. Arenas, Effect of growth orientation and heat treatment on the corrosion properties of AlSi10Mg alloy produced by additive manufacturing, ***J. Mater. Res. Technol.*** 18 **(2022)** 5325. https://doi.org/10.1016/j.jmrt.2022.05.021

[40] F. Bosio, C. Phutela, N. Ghisi, A. Alhammadi, N.T. Aboulkhair, Tuning the microstructure and mechanical properties of AlSi10Mg alloy via *in situ* heat treatments in laser powder bed fusion, ***Mater. Sci. Eng.*** A. 879 **(2023)** 145268. https://doi.org/10.1016/j.msea.2023.145268

[41] J. Fiocchi, A. Tuissi, C.A. Biffi, Heat treatment of aluminium alloys produced by laser powder bed fusion: ***A review, Mater. Des.*** 204 **(2021)** 109651. https://doi.org/10.1016/j.matdes.2021.109651

[42] I.S. Munoz, I. Roveda, A. Kupsch, B.R. Müller, G. Bruno, Synchrotron X-ray refraction detects microstructure and porosity evolution during *in situ* heat treatments, ***Mater. Sci. Eng.*** A. 838 **(2022)** 142732. https://doi.org/10.1016/j.msea.2022.142732

[43] S. Bagherifard, N. Beretta, S. Monti, M. Riccio, M. Bandini, M. Guagliano, On fatigue strength enhancement of additive manufactured AlSi10Mg parts mechanical and thermal post

processing, ***Mater. Des.*** 145 **(2018)** 28. https://doi.org/10.1016/j.matdes.2018.02.055

[44] U. Zerbst, G. Bruno, J.Y. Buffière, T. Wegener, T. Niendorf, T. Wu, X. Zhang, N. Kashaev, G. Meneghetti, N. Hrabe, M. Madia, T. Werner, K. Hilgenberg, M. Koukolíková, R. Procházka, J. Džugan, B. M'ller, S. Beretta, A. Evans, R. Wagener, K. Schnabel, Damage tolerant design of additively manufactured metallic components subjected to cyclic loading: State of the art and challenges, ***Prog. Mater. Sci.*** 121 **(2021)** 100786. https://doi.org/10.1016/j.pmatsci.2021.100786

[45] T.H. Becker, P. Kumar, U. Ramamurty, Fracture and fatigue in additively manufactured metals, ***Acta Mater.*** 219 **(2021)** 117240. https://doi.org/10.1016/j.actamat.2021.117240

[46] N. Sanaei, A. Fatemi, Defects in additive manufactured metals and their effect on fatigue performance: A state of the art review, ***Prog. Mater. Sci.*** 117 **(2021)** 100724. https://doi.org/10.1016/j.pmatsci.2020.100724

[47] U. Zerbst, K. Hilgenberg, Damage development and damage tolerance of structures manufactured by selective laser melting – a review, ***Proc. Struct. Integrity.*** 7 **(2017)** 141. https://doi.org/10.1016/j.prostr.2017.11.071

[48] P. Foti, N. Razavi, A. Fatemi, F. Berto, Multiaxial fatigue of additively manufactured metallic components: A review of failure mechanisms and fatigue life prediction methodologies, ***Prog. Mater. Sci.*** 137 **(2023)** 101126. https://doi.org/10.1016/j.pmatsci.2023.101126

****

News Updates National

Centre to support setting up of pilot projects using Green Hydrogen for steel making

The centre will aid research and development (R&D) projects to set up pilot plants for production and utilisation of green hydrogen in the iron and steel making processes, the steel ministry has said.

It said Rs. 455 crore has been earmarked under the National Green Hydrogen Mission to support the domestic steel industry's endeavours to find scalable uses of hydrogen produced using environmentally sustainable practises. This low-environment-footprint hydrogen is called green hydrogen to signify its superior acceptability.

Tightening regulatory regimes around the world threaten to make steel produced in India uncompetitive due to the levy of higher duties by the European countries. These penalties are proposed to be imposed on steel manufactured using conventional practises that have higher emissions and are contributing to global warming.

Most steel around the world, including in India, is made using direct reduction of iron, which is the chemical removal of oxygen from iron ore. This activity is carried out in a blast furnace, usually with the help of coking coal.

To reduce emissions from this exercise, efforts are being made globally to use green hydrogen instead of coal. The domestic steel industry has sought financial support to undertake this transition.

The Economic Times (2.6.23)

India's coal production grows 7.10 pc to 76.26 million tonne in May

Domestic coal production was 7.10 per cent higher year-on-year at 76.26 million tonne (Mt) in May. India had produced 71.21 Mt coal during the same month in 2022, the coal ministry said in a statement.

"Ministry of Coal has achieved a remarkable feat with a substantial surge in overall coal production during May 23, reaching 76.26 Mt surpassing May 22 of 71.21 Mt, representing an increase of 7.10 per cent," it said.

The cumulative coal production in April-May FY24 jumped to 149.41 Mt from 138.41 Mt in the year-ago period. Last month, Coal India Ltd (CIL) alone produced 59.94 Mt coal, up 9.54 per cent over 54.72 Mt in May 2022.

With an increased first-mile connectivity infrastructure, coal dispatch last month grew 5.70 per cent to 82.22 Mt from 77.79 Mt in May 2022. First-mile connectivity refers to the transportation of coal from pitheads to dispatch points.

The total coal stock as of May 31, 2023 is 112.41 Mt as compared to 82.97 Mt on May 31, 2022, a growth of 35.48 per cent.

The Economic Times (2.6.23)

Steel Minister Scindia inaugurates SAIL's Rs 149-cr beneficiation plant in Chhattisgarh

Union Steel Minister Jyotiraditya M Scindia inaugurated a Rs 149-crore beneficiation project of Steel Authority of India Ltd (SAIL) at Kanker in Chhattisgarh. The minister virtually inaugurated the SAIL's Silica Reduction Plant set up at the company's Dalli iron ore mines.

In his address, Scindia said the new plant is an important milestone as it will help the steel maker utilise the low-grade ore from the Dalli mines through the beneficiation process.

Around 80 per cent of the reserves of the iron ore mine has been utilized, he said adding certain issues were coming in the utilisation of the remaining 20 per cent reserve like the Fe or iron content was below 60 per cent and silica content was as high as 10 per cent. The plant will improve the Fe content to 62-64 per cent and bring down the silica content to 2-3 per cent.

SAIL Chairman Amarendu Prakash said that there was a need to refine iron ore of size less than 1 mm to achieve the desired grade for effective usage in the blast furnace at the company's Bhilai Steel Plant (BSP), and the company plans to set up more such projects to utilise low-grade ores.

The Economic Times (23.6.23)

****

रक्षा अनुसंधान एवं विकास संगठन
रक्षा मंत्रालय, भारत सरकार
DEFENCE RESEARCH & DEVELOPMENT ORGANISATION
Ministry of Defence, Government of India

Aeronautics Research & Development Board

Vision

Make India technologically strong by establishing world class cutting edge aeronautical science and technology base to provide our Defence, Space and Civil Aviation sectors a decisive edge by equipping them with internationally competitive systems and solutions.

Mission

To encourage and fund basic and applied research in pertinent scientific disciplines directly relevant to our aeronautical systems needed for future by enabling and supporting emerging talents, particularly in academic and research institutions to create and evolve a potential knowledge-base system applicable to future aeronautics needs of the country.

Charter

- To formulate research, design and development programmes in aeronautics and allied sciences, keeping in view future needs of the country specifically with respect to aircraft, helicopter, missiles and all other airborne vehicles.
- To implement such programmes through appropriate institutions and individuals by sponsoring research, design and development projects, creating/ improving infrastructure facilities deemed necessary, while ensuring that they are suitably monitored.
- To promote in all possible ways such educational and training programmes as may be considered necessary for ensuring that adequate manpower of requisite quality becomes available to various aeronautical organizations in the country.
- To promote all relevant R&D activities in the country through appropriate scientific meetings, provisions of support for participation of Indian and foreign scientists in such meetings, conduct of relevant competitions as well as other training and visiting programmes within India and abroad as may fall within the scope of the programmes mentioned at sub para (a) above.
- Dissemination of appropriate technical information through journals and documents, encouragement of individual and collective efforts and nurturing of young talent by institutions with suitable awards, scholarships etc. Organization of necessary centralized services related documentation, software, data-link etc. and in all such other ways that the Board may determine from time to time.

Panels & Chairmen (2017-2022)	
Aerodynamics Panel **Dr S Pandian** Prof. Vikram Sarabhai Distinguished Professor & Ex- Director & DS, SHAR	**Propulsion Panel** **Dr V Ramanujachari** National Centre for Combustion Research & Development (NCCRD), IIT Madras, Chennai
Aerospace Resources Panel **Dr N Eswara Prasad** OS & Ex-Director, DMSRDE (DRDO), Knp.-13	**UNMANNED AERO SYSTEMS PANEL** **Shri PS Krishnan** DS & Ex-Director, ADE, Bangalore-560075
Materials & Manufacturing Panel **Dr DK Das, Scientist H** Group Head (DSG), DMRL (DRDO) Hyd. - 58	**Structures Panel** **Dr Makarand Joshi** Scientist G, R&DE (E), DRDO, Pune-411015
GTMAP **Prof. Amol A Gokhale, IITB, Chairman**	**Systems / Systems Engineering Panel** **Shri APVS Prasad** Scientist H, CE, CEMILAC, DRDO, Bangalore

Chapter Activities — Vijayanagar, Kolkata, Hyderabad

Vijayanagar Chapter

The Indian Institute of Metals, Vijayanagar chapter has been very active in conducting lectures and various events to promote science and technology of steel making. These events help shape employees into well-rounded individuals, foster love for learning and fuel the thirst for knowledge. In a bid to promote scientific knowledge and engage the community in a fun and educational event, IIM Vijayanagar Chapter conducted Interdepartmental Metals and Materials Quiz 2023 during the months of May-June 2023.

Participants from various departments and working backgrounds came together to showcase their knowledge and passion for all things metallic. Quiz was conducted in two phases. In first phase a Semifinal round conducted on 20th May 2023 where 8 departmental teams battled out for the top 4 positions. In the second phase Grand Finale was organised on 24th June 2023 with 4 teams fighting for the top position. Each round featured questions of varying difficulty, ensuring that participants were tested on their comprehensive understanding of metals and materials. Finally team PDQC, CSD and Services were the top scorer and won the 1st Prize, Team R&D, TQM, Environment and Energy Management won the second Prize and Team Coke Oven and Iron Making won the 3rd prize. With multiple rounds of challenging questions and a competitive atmosphere, the event proved to be a stimulating experience for all involved.

The quiz was addressed by Mr. L R Singh COO-Vijayanagar works and Secretary IIM Vijayanagar Chapter. He highlighted that quiz event like this is not merely a platform to showcase our knowledge, but also an opportunity to celebrate curiosity, critical thinking, and the pursuit of knowledge. There were audience questions and prizes for the same, which brought good participation from all over the plant. The quiz concluded with awards distribution to the participant winners and audience prize winners. Beyond the competitive nature of this event, let us remember the true essence of quizzing: collaboration and teamwork. It also helps us lean the subject beyond our boundaries of work. The success of this metals and materials quiz has left the JSWites motivated to organize similar events in the future.

Glimpse of 'Metals and Materials Quiz 2023'

Kolkata Chapter

The Annual General Meeting of IIM Kolkata Chapter was convened on 30th May, 2023 at Metal House, IIM Head Office. The new Executive Committee for the year 2023-24 was elected which is as follows :

- Chairman ➢ Shri Sudip Kr. Basak
- Secretary ➢ Shri Surajit Kumar Dutta
- Treasurer ➢ Shri Arnab Banerjee

Hyderabad Chapter : Industry-Institute Summit-2023

The Department of Metallurgical and Materials Engineering, Mahatma Gandhi Institute of Technology (MGIT), in association with The Indian Institute of Metals, Hyderabad Chapter organised an Industry-Institute Summit at the premises of MGIT on June 5, 2023. The summit was attended by the entrepreneurs of several metallurgical industries located in and around Hyderabad. They have made detailed presentations about the infrastructural facilities existing in their organizations. The internship and employability prospects in their Industries have been dealt at length. They have expressed their willingness to collaborate with the Department in due course of time to execute joint projects. The industrialists answered many questions raised by students during the panel discussion. Prof. Chandra Mohan Reddy, Principal, MGIT, Dr. K. Ramanjaneyulu, Head of the Dept., MME, MGIT, Dr. K. Satyanarayana, Parisodhana Technologies, Mr. Siva Rama Prasad, MSME, Mr. Surya Prakash Rao, Associated Engineering Services, Dr. Pavan, Eaton, Mr. Varun, Saideepa Rockdrills, and Mr. Sharath, Fusion Heat Treaters were among the dignitaries attended during the event. The members of IIM Students Chapter at MGIT were benefitted from the intense discussions and interactions they had with the industrialists.

Industry-Institute Summit-2023 @ MGIT, Hyderabad

****

Member in the News Dr Mayur Vaidya

Dr. Mayur Vaidya, a Life Member of IIM, has been awarded prestigious INSA (Indian National Science Academy) Medal for Young Scientist (2022). The award carries a medal, certificate, and honorarium of Rs. 1,00,000. The certificate and medal were presented during the General Body Meeting of the Academy held on 9 May 2023 at the Academy premises. The recognition was given for his very significant contribution of deciphering the mechanism of diffusion in high entropy alloys (HEA). The understanding developed through his work will help in the development of better HEAs for novel technological applications. Dr. Mayur Vaidya is currently a faculty at the Department of Materials Science and Metallurgical Engineering at Indian Institute of Technology Hyderabad.

****

Achievements NMA 2022

Ministry of Steel
National Metallurgist Awards for the year 2022

The Ministry of Steel announced the NMA 2022 awards mentioned against their names through the notification issued through (S-20026/2/2022-Tech), New Delhi, on 18.04.2023.

S. No.	Recipient Name	Award Category
1.	Dr. Kamachi Mudali Uthandi	Lifetime Achievement Award
2.	Dr. Rameshwar Sah	Award in R&D in Iron & Steel Sector
3.	Dr. Debashish Bhattacharjee	National Metallurgist Award
4.	Dr. Niloy Kundu	Young Metallurgist (Environment) Award
5.	Dr. Agilan Muthumanickam	Young Metallurgist (Metal Science) Award

The Indian Institute of Metals congratulates the award recipients.

****

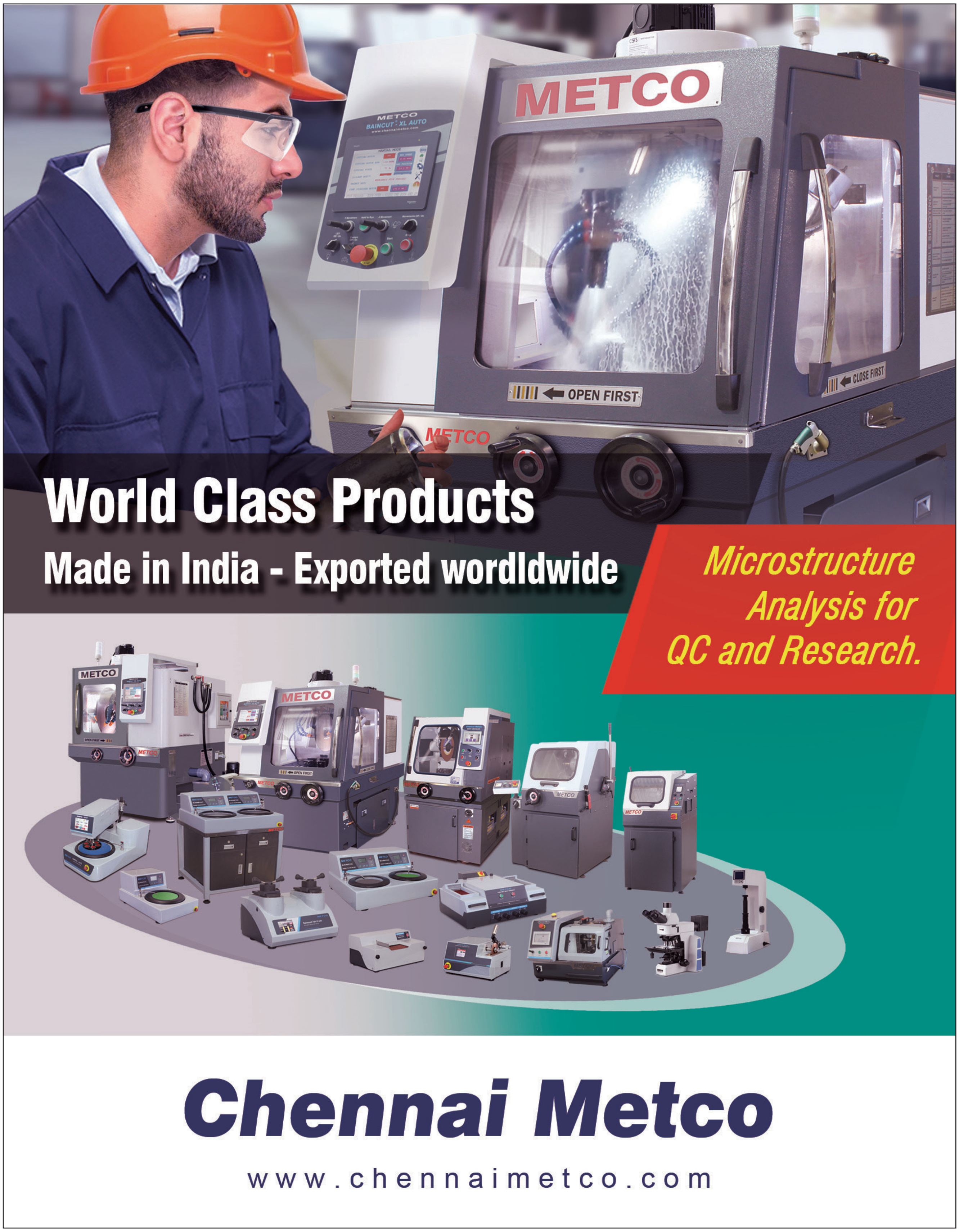
METCO
OPEN FIRST
CLOSE FIRST
World Class Products
Made in India - Exported worldldwide
Microstructure
Analysis for
QC and Research.
METCO
Chennai Metco
www.chennaimetco.com

Monthly Summary on Iron and Steel June - 2023

1. Performance of Steel sector during Q1:FY24 has been encouraging. The production of crude steel at 33.63 million tonnes (Mt), finished steel at 32.41 Mt and consumption of finished steel at 30.29 MT during Q1:FY24 was the highest in corresponding period of last five years (Graph-1). The month-wise production and consumption (Graph-2) indicates a mixed trend with month-on-month fluctuations and that the production of Crude Steel increased in June ’23 over their respective levels in May ’23 and production of finished steel and consumption of steel decreased in June ’23 over their respective levels in May ’23.

i. Production of crude steel in June ’23 at 11.28 Mt increased by 13.7% over CPLY and 1.0% by M-o-M.

ii. Production of finished steel in May ’23 at 10.52 Mt increased by 11.9% over CPLY but decreased by 4.4% over the previous M-o-M.

iii. Consumption of finished steel in May ’23 at 9.88 Mt increased by 13.8% over CPLY but decreased by 5.3% over the previous M-o-M.

iv. Inventories of the finished steel with the steel producing companies at 12.07 Mt at the end of June ’23 increased by 5.5% M-o-M and 42.0% over CPLY.

2. *Among the steel CPSEs, SAIL achieved its best ever April-June (Q1) production of Hot Metal, Crude Steel and Saleable Steel in any year. NMDC also achieved its best ever Q1 production and sales performance since inception. Similarly, MOIL also recorded its best ever Quarterly production performance in Q1: 2023-24.* During the month of June ’23, among the steel producing CPSEs, Steel Authority of India (SAIL) registered a decrease in production of Hot Metal over the previous month (M-o-M) but increased over CPLY. The production of Crude Steel and Saleable steel registered an increase in production over the previous month (M-o-M) and over the corresponding period last year (CPLY). Rashtriya Ispat Nigam Limited (RINL) registered an increase in production of liquid steel, hot metal and crude steel over the previous month (M-o-M) but registered a decrease in production of liquid steel and hot metal but the production of crude steel remained constant over CPLY. The production of saleable steel by RINL during June ’23 increased over the previous month (M-o-M) and over CPLY. Production of iron ore by National Mineral Development Corporation (NMDC) witnessed a decrease over previous month but increased over June ’22. The ore production by SAIL during June ’23 was lower than previous month and over CPLY. Similarly, the production of ore by MOIL was lower over previous month but higher over CPLY. The detailed performance of the Steel CPSEs is as below:

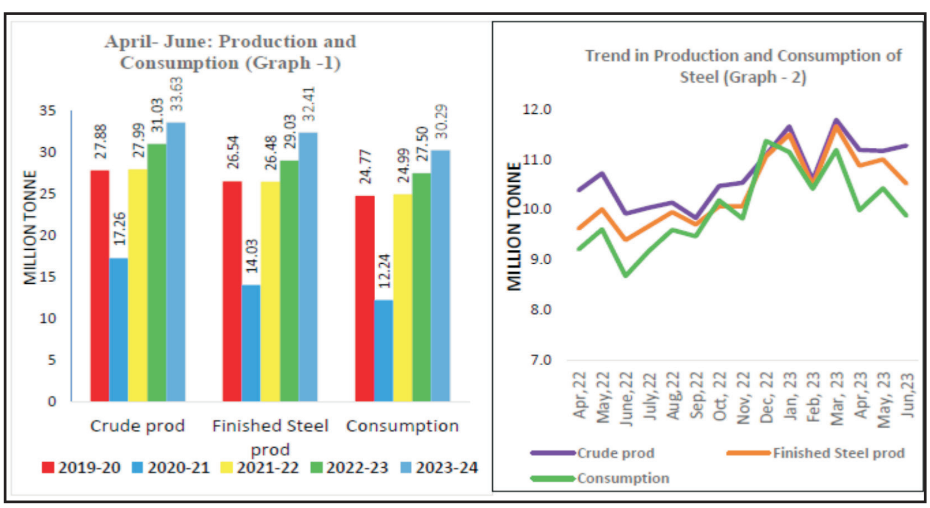

i. During June ’23, SAIL produced 16.77 lakh metric tonne (LMT) of Hot Metal recording a decrease of 1.1% over previous month (MoM) but increase by 12.1% over CPLY. During June ’23, SAIL produced 15.66 LMT of Crude Steel and 14.82 LMT of Saleable Steel recording an increase of 0.1% and 0.7% respectively over previous month (MoM) and 12.3% and 11.4% respectively over CPLY. The cumulative production of SAIL during Q1:FY24 for Hot Metal at 50.37 LMT, Crude Steel at 46.67 LMT and Saleable Steel at 44.05 LMT registered an improvement of 7.3%, 7.8% and 8.0% respectively, over CPLY. During the month, SAIL produced around 27.35 LMT of iron ore recording a decrease of 8.3% M-o-M and 3.3% over CPLY. The cumulative production of iron ore by SAIL during Q1:FY24 at 84.64 LMT was 0.4% lower than CPLY.

ii. Production of iron ore by NMDC at 34.83 LMT in June ’23 registered a decrease of 6.1% M-o-M but increased by 35.7% over CPLY. The cumulative production of iron ore by NMDC during Q1:FY24 at 107.03 LMT increased by 20.0% over CPLY. Sale of iron ore by NMDC at 41.04 LMT in June ’23 was higher by 13.4% M-o-M and by 116.2% over CPLY. During Q1:FY24, sale of iron ore by NMDC at 111.55 LMT was high by 45.6% over CPLY.

iii. During the month Kudremukh Iron Ore Company Limited (KIOCL) produced 1.45 LMT of Pellets which was higher by 28.3% M-o-M and 383.3% over CPLY. KIOCL sold 2.85 LMT of Pellets which was higher by 285.1% M-o-M and 481.6% over CPLY. During Q1:FY24, production of Pellets by KIOCL at 4.88 LMT recorded an increase of 13.8% and its sales at 5.26 LMT recorded an increase of 96.3% over CPLY.

iv. During June ’23, production of Manganese ore by Manganese Ore (India) Limited (MOIL) at 1.52 LMT was lower by 0.7% M-o-M but higher by 36.9% over CPLY. Sale of Manganese ore by MOIL during June ’23 at 1.45 LMT was lower by 5.2% M-o-M but higher by 5.1% over CPLY. During Q1:FY24, production of Manganese ore at 4.36 LMT was higher by 35.4% and its Sale at 3.96 LMT was higher by 39.4% over CPLY.

v. During June ’23, RINL’s production of Liquid Steel was 3.76 LMT, Hot Metal at 3.82 LMT and Crude Steel at 3.60 LMT, which was 52.9%, 43.1% and 52.5% higher than its production in May ’23 respectively but lower by 0.3% and 0.3% over CPLY for Liquid Steel and Hot Metal respectively and remain constant for Crude Steel. During the month of June ’23, the production of Saleable Steel by RINL at 3.39 LMT, which was 43.0% higher than its production in May ’23 and by 6.3% over CPLY. During Q1:FY24, the production of Liquid Steel was 10.36 LMT, Hot Metal 10.68 LMT and Crude Steel 9.95 LMT was 1.7%, 4.0% and 1.3% lower than their respective productions during CPLY. However, during Q1:FY24, the production of Saleable Steel by RINL was 9.39 LMT, which was 24.0% higher than their respective productions during CPLY.

3. The CAPEX by Steel CPSEs in June ’23 at Rs. 747.21 crore was 8.1% higher over the previous month (M-o-M) but was 5.8% lower than CAPEX in CPLY. The CAPEX by steel CPSEs for Q1:FY24 at Rs. 1,842.31 crore was 8.2% higher than CAPEX during CPLY and it was 7.3% of the BE for the FY ’24. The CAPEX by steel CPSEs is regularly monitored by the Ministry and steel CPSEs are being encouraged and directed to ensure achievement of CAPEX and expedite spending.

4. Hon’ble Steel Minister (HSM) inaugurated the Silica Reduction Plant at Steel Authority of India Limited's (SAIL) Bhilai Steel Plant's Dalli Mines, from New Delhi, on 23rd June, 2023. HSM mentioned that the steel sector has played a prominent role in the growth story of India through employment generation and providing foundational infrastructure. He said that the government is working fast on the infrastructure, due to which the consumption has increased from 77 Mt to 120 Mt and per capita steel consumption, which was 60 kg in 2014 has now reached 87 kg, recording an increase of 50 percent. In line with the vision of Aatmanirbharta, India has now emerged as a net exporter of Steel from being a net importer, 9 years back.

5. Ministry of Steel has introduced Steel Quality Control Order (QCO) thereby banning sub-standard/ defective steel products both from domestic & imports to ensure the availability of quality steel to

the industry, users and public at large. As per the Order, it is ensured that only quality steel conforming to the relevant BIS standards are made available to the end users. As on date 145 Indian Standards have been notified under the Quality Control Order covering carbon steel, alloy steel and stainless steel. Out of these, QCO on 144 Indian Standards have been enforced. The draft QCO for inclusion of six additional Indian Standards pertaining to the iron & steel sector has been uploaded in Ministry of Steel's Website on 02.06.2023 and on WTO website vide regular TBT notification no. G/TBT/N/IND/278 dated 14.06.2023 for comments of the stakeholders. As per WTO-TBT mandate, the final date for comments on the said notification is 60 days from the date of notification in WTO website i.e. 13.08.2023.

6. Ministry of Steel got several requests from the importers/ applicants seeking clarification on the applicability of the certain imported steel grades from the purview of the Quality Control Order, on the ground that these are complying with foreign standards and no equivalent Indian Standards exist. To address this issue, a Technical Committee, comprising members from the BIS, steel producers & end users, was constituted to examine the applications and clarify whether the imported steel grades are falling under the purview of the QCO or otherwise. Meetings of the Technical Committee were held on 6th June 2023, wherein 811 applications for clarification on the applicability of QCO on the imported steel grades were examined.

7. Presently, there are eight ongoing projects of steel CPSEs (SAIL-5, NMDC-3) uploaded on the OCMS portal of MoSPI. The total cost of these projects is Rs. 30,201 crores and an expenditure of Rs. 26,602.08 crores (88.1%) has been incurred till June '23.

8. There are Nine National Infrastructure Pipeline (NIP) Projects related to slurry pipelines of various steel companies having a total cost of Rs. 26,628 crore uploaded on IIG/NIP Portal and an expenditure of Rs. 3,519 crore has been incurred on these projects till June '23. Secretary Steel reviewed the major CAPEX Projects, Project Management and Procurement Procedures of all the CPSEs on 19.06.2023 & 20.06.2023 and directed them to expedite the progress of projects.

9. The status of pending payments to MSMEs by CPSEs of the Ministry is being monitored on weekly basis to ensure payments to them within the 45 days' time limit for such payments. Payment of Rs. 647.74 crores was made by Steel CPSEs to MSMEs during June '23 which is 7.8% higher than payments made during CPLY and 6.4% lower than M-o-M. During Q1:FY24, Steel CPSEs have made payment of Rs. 1,969.06 crore to MSMEs, which is 18.0% higher than Rs. 1,668.45 crore made during CPLY.

10. **Export-Import Scenario:** During the month of June '23, imports of finished steel increased but the exports decreased as compared to previous month as shown in graph-3.

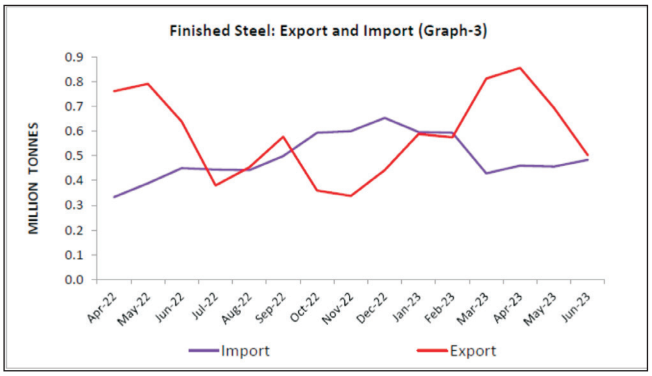

i. In June '23, India was a net exporter of finished steel. Export of finished steel was 5.02 Lakh Metric Tonne (LMT) in June '23, which decreased by 27.6% M-o-M and by 21.3% over June '22. Imports of finished steel was 4.84 LMT in June '23, showing an increase of 5.9% M-o-M and 7.6% over June '22. During Q1:FY24, exports at 20.50 LMT declined by 6.4% while imports at 14.01 LMT increased by 19.5% over CPLY.

ii. Share of China, Japan, Vietnam, Saudi Arabia, Russia, Nepal and USA increased in total steel import of India in June '23 as compared to June '22 while share of Korea, Germany and Sweden declined over this period as may be seen from the following graphs 4 & 5:

iii. Share of Italy, Nepal, UK, Mexico, Russia and Portugal increased in total steel export from India in June '23 as compared to June '22 while share of UAE, Belgium, Vietnam and Spain declined over this period as may be seen from the following graphs 6 & 7:

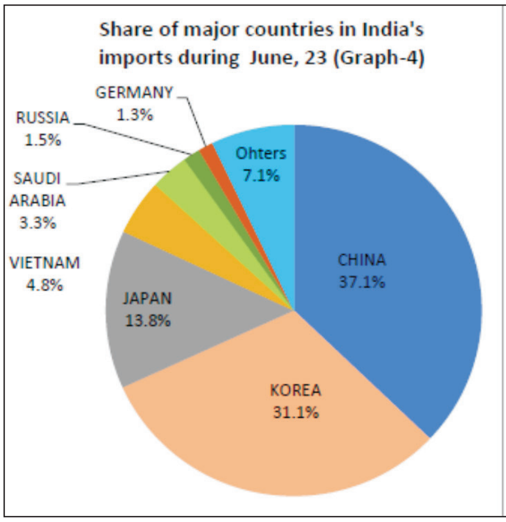

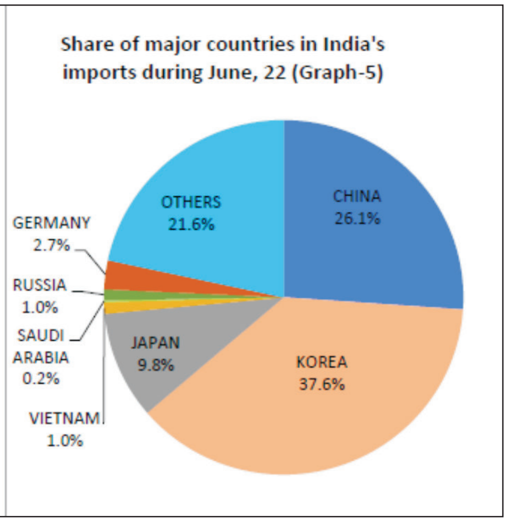

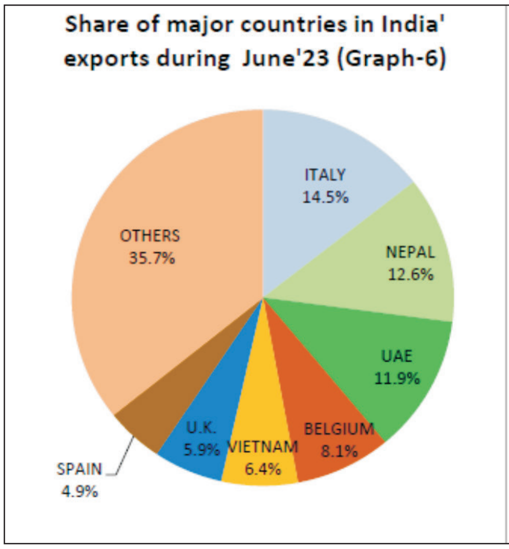

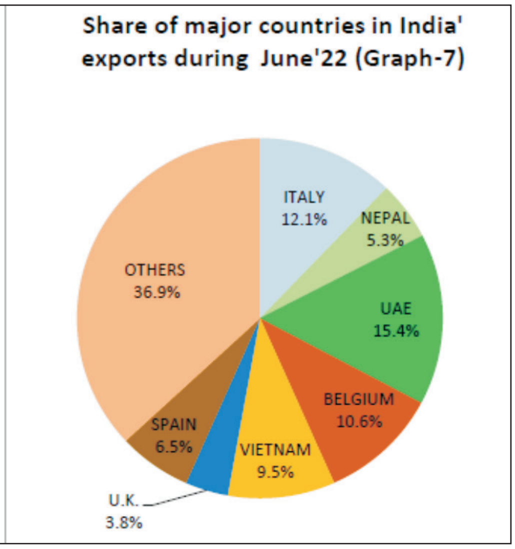

11. The prices of iron ore declined during April '22 to July '22. However, after December '22 it has shown some recovery and declining since April '23 as may be seen from the graph-8.

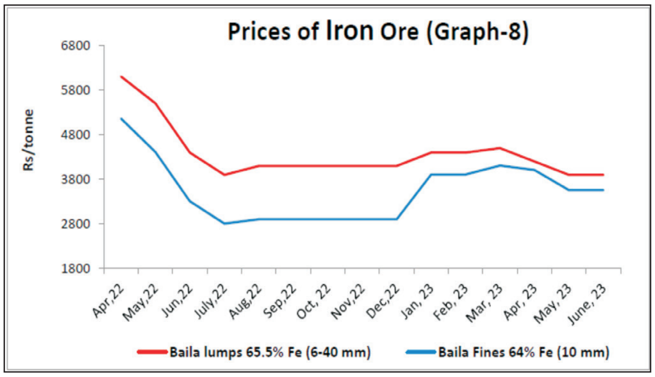

i. During the month of June '23, prices of iron ore lump and fines was Rs. 3,900/tonne and Rs. 3,560/tonne, which remained constant over their respective prices in May '23.

ii. The prices of HCC Coking coal f.o.b. Australia have increased from USD 224/tonne on 31.05.2023 to USD 233/tonne on 30.06.2023.

iii. The prices of steel (TMT, HRC and CRC) peaked in March '22 on account of Russia-Ukraine war. After that steel prices have moderated till December '22 due to both global and domestic factors. The prices of TMT, HRC and CRC have declined in June '23 over June '22 as may be seen from the graph-9.

iv. The retail prices of TMT (10mm), HRC (2.50mm) and CRC (0.63mm) in Mumbai market stood at Rs.62,970/tonne, Rs. 64,910/tonne and Rs. 72,020/tonne on 30th June '23, recording a decline of 2.5%, 4.3% and 1.6% respectively over prices on 31st May '23.

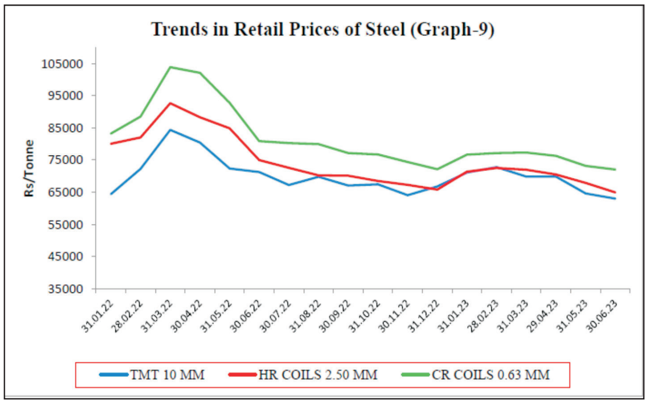

12. The global production of crude steel decreased by 5.1% in May '23 over CPLY mainly due to decrease in production in China, Japan, USA, South Korea, Turkey and Brazil. Among the major steel producing countries (with production of over 1 million tonnes for the month), India, Russia, Iran and Germany recorded an increase in production in May '23 over May '22. During January-May '23, India performed the best among major steel producing countries and produced 563.93 LMT of crude steel, which was higher by 5.7% over CPLY. As for the share of major steel producing countries in the global production of crude steel, it is seen that share of India, USA, Russia, South Korea, Iran and Germany increased during May '23 while that of China and Turkey declined and share of Japan and Brazil remained constant during this period as may be seen from the following graphs 10 & 11.

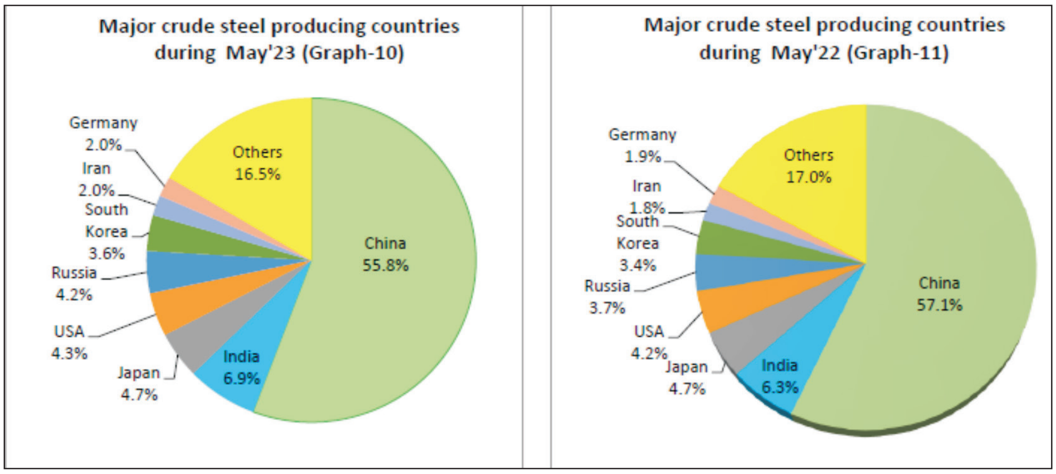

Source : https://steel.gov.in/

****

Seminars & Conferences — Indian Mining Minerals Conclave 2023

The Associated Chambers of Commerce and Industry of India (ASSOCHAM) hosted Indian Mining and Minerals Conclave & Business Excellence Awards 2023 on 30th June, 2023 in Kolkata. The Indian Mining & Minerals Conclave served as a platform for the senior government officials, top industry leaders, MSMEs, Startups, etc. from the mining sector to discuss policies, practices, business developments, management strategies, etc. to strengthen the entire ecosystem of minerals and mining, including the mining machinery manufacturing business. ASSOCHAM & ICRA jointly released a knowledge report on the industry. The Indian Institute of Metals (IIM) was the association partner and Shri Bhaskar Roy, Acting Secretary General, IIM attended the event.

Eminent dignitaries & speakers such as Shri Anurag Srivastava, IAS, Secretary, Department of Industry Commerce & Enterprises, Govt. of West Bengal, Mr. Arun Kumar Shukla, Chairman & Managing Director, Hindustan Copper Ltd., Mr. Sanjeev Kumar Singh, Director(Mining), Hindustan Copper Ltd., Mr. Ritabrata Ghosh, Vice President & Sector Head, Corporate Sector Rating, ICRA Limited, Mr. Sunil Chaturvedi, Group Chairman, Gainwell Commosales Pvt. Ltd., Mr. Sanjiv Ganeriwala, Jt. Managing Director, Maheshwari Mining Pvt. Ltd., Mr. Soham Misra, Chairman, ASSOCHAM Iron & Steel Sub Council East was present to enlighten the audience.

Chief Guest, Shri Anurag Srivastava, IAS, Secretary, Department of Industry Commerce Enterprises, Govt. of West Bengal, said "Bengal stands one fifth in India's total mineral reserve. The Deocha Pachami coal block will soon be operational and is Asia's biggest. He also shared information with regard to Oil sector, and state plans of development. With the rapid infrastructural development of gas pipelines in the state, our city will soon have 38 lakh PNG connections,".

The Government and industry stakeholders are always on a continuous endeavor to develop the mining fraternity to make it more productive, safer, encourage further innovation and make it more sustainable for the future as mining has always been the epicenter for industrial development and growth at national and international level.

On the occasion of the Minerals and Mining Conclave, ASSOCHAM organised The Business Excellence Awards to acknowledge and celebrate the achievements of Corporates and MSMEs (including Startups) and the Best Business practices followed by them, leading to business transformation and sustainability. The Business Excellence Awards are the highest recognition, which has a significant and positive impact.

****

Upcoming Conferences National and International

1. **MIMA-3 International Conference on**
   Materials, Inspection, Monitoring and Assessment
   Electricity Generation through Fossil, Nuclear and Renewables –
   Materials, Inspection, Monitoring, Digitalisation & Flexibility

   Dt : 17 – 19 October 2023

   Venue: Woburn House, 20 Tavistock Square, London

   Website: www.woburnhouse.co.uk

   Registration : enquiries@etd-consulting.com

2. **International Seminar on**
   Strategies for Sustainable Growth and Profit Maximization for Steel Plants in India

   Dt: 16th October, 2023, Monday

   Venue: ITC, Sonar (PALA), Kolkata, India

   Website: www.steeltech-india.com

   Mr. BP Sarkar (Convenor), Email: sarkar.bp@gmail.com ; info@steeltech-india

3. **Third International Conference on**
   Structural Integrity (ICONS - 2023)

   Dt: August 23-25, 2023

   Venue: Convention Center, Four Points by Sheraton, Mamallapuram, Tamil Nadu, India.

   Organisers: Indira Gandhi Centre for Atomic Research (IGCAR), Kalpakkam and Society for Failure Analysis Chennai Chapter.

   Co-organizers: Indian Institute of Technology Madras (IITM)-Chennai, Indian Society for Non-destructive Testing (ISNT)-Kalpakkam chapter, The Indian Institute of Metals (IIM)-Kalpakkam chapter and Indian Structural Integrity Society (InSIS).

   Topics to be covered:

   • Mechanical Behaviour of Materials • Fatigue and Fracture Mechanics • Creep and Creep-Fatigue Interaction • High Strain Rate Loading • Small Specimens Test Methods • Fretting and Multi-axial fatigue • Fracture Mechanics based Design • Computational Mechanics • Micromechanics of Fracture and Damage • Steel and Concrete Structures • Composites, Bio and Nano Materials • Structural Materials and Weldment • NDE and Structural Health Monitoring • Failure Analysis • Reliability and Structural Integrity Assessment • Fitness for Service and Remaining Life Assessment • LBB Analysis • Regulatory Aspects • Life of Nuclear Structures, Aerospace and Automobile Applications • Offshore and Marine Structure Contact: Chairman, Local Organizing Committee, Dr. M Vasudevan: dev@igcar.gov.in ICONS Office: icons@igcar.gov.in; Ph.: +91 44 27480003; Website: https://www.icons2023.in

****

Production (unit : Lakh Tonnes)

	May'23	Apr'23	Mar'23	2022 - 23	2021 - 22
ALUMINIUM					
National Aluminium Co Ltd	0.40	0.39	0.40	4.60	4.60
Hindalco Industries Ltd*	1.13	1.09	1.13	13.22	12.94
Bharat Aluminium Co. Ltd	0.49	0.48	0.49	5.69	5.80
Vedanta Ltd	1.49	1.43	1.48	17.22	16.92
TOTAL	**3.51**	**3.39**	**3.50**	**40.73**	**40.26**
*Renukoot, Hirakund, Mahan, Aditya					
ZINC (One major producer)					
Hindustan Zinc Ltd	**0.70**	**0.70**	**0.77**	**8.21**	**7.76**
COPPER (Cathode)					
Hindustan Copper Ltd	0	0	0	0.000073	0.62
Hindalco (Birla Copper)	0.18	0.28	0.36	4.07	3.59
Vedanta Ltd.	0.13	0.08	0.10	1.48	1.25
TOTAL	**0.31**	**0.36**	**0.46**	**5.55**	**4.85**
LEAD					
Hindustan Zinc Ltd	**0.18**	**0.17**	**0.19**	**2.11**	**1.91**

Source : https://mines.gov.in/

Prices in India (as on 30th June, 2023)

(Mumbai Local Price in Rs. / kg)

Product	Rs. / kg	Product	Rs. / kg
Copper Armature	697	Aluminium Ingot	202
Copper Cathod	726	Aluminium utensil	167
CC Rod	736	Zinc Ingot	216
Copper Cable scrap	711	Lead ingot	185
Brass Sheet Scrap	506	Tin Ingot	2345
Brass Honey Scrap	488	Nickel Cathod	1728

Source : https://mtlexs.com/